OPTIMIZATION OF TORREFACTION ON TORREFIED BIOCHAR FROM OIL PALM EMPTY FRUIT BUNCHES FOR POTENTIAL BIOMASS ENERGY

by

ROSE NADIAH BINTI ABU HASAN

A report submitted in fulfillment of the requirements for the degree of Bachelor of Applied Science (Sustainable Science)

FACULTY OF EARTH SCIENCE
UNIVERSITI MALAYSIA KELANTAN

2020

DECLARATION

I declared that this thesis entitled "Optimization of Torrefaction on Torrefied Biochar from Oil Palm Empty Fruit Bunches (OPEFB) for Potential Biomass Energy" is the result of my own research except as cited in the references. This thesis has not been accepted for my degree and is not concurrently submitted in candidature of any other degree.

Signature : ______________________________

Name : ROSE NADIAH ABU HASAN

Date : 6 JANUARY 2020

ACKNOWLEDGEMENT

Thanks to Allah SWT, whom with His willing giving me the chance and opportunity to complete the Final Year Project successfully. I would like to express the deepest appreciation to my supervisor, Ts. Dr. Mohamad Faiz bin Mohd Amin, who gives guidance and information regarding to my Final Year Project. Without his guidance and persistent helps, the Final Year Project would not have been possible.

I would like to thank to Mr Mohd Sukhairi Mat Rasat as my research team leader and Dr Siti Saniah Ab Karim who had guided me in a lot task during the entire process of this thesis writing and design experiment. I would also want to thanks the lecturers and staffs of Faculty of Earth Science for their advise and contribution during completing this report.

Deepest appreciation for my late parents, family members, and team member Nur Adlin Aziz for giving me encouragement and support for the report completion from the beginning and till the end of the process. Special thanks to all my friends have have been helping me and contributed to the completion of the Final Year Project until the very end.

Optimization of Torrefaction on Torrefied Biochar from Oil Palm Empty Fruit Bunches (OPEFB) for Potential Biomass Energy

ABSTRACT

The worldwide demand for energy and energy use is increasing rapidly. The biomass resource was chosen as a renewable energy sources based on the abundance of oil palm waste generated monthly. The aim of this study is to find an optimal value of torrefection process on the torrefied biochar from the oil palm empty fruit bunches (OPEFB) in order to produce biomass energy source by using the Box-Behnken design of Response Surface Methodology (RSM). In this study, OPEFB were torrefied based on the three dependent variables which are particle size of 250-750 µm, holding temperature of 200-300°C and residence time of 30-90 minutes. Torrefied biochar were being optimized in regards of six independent variables which were mass yield, calorific value, fixed carbon, moisture content, volatile matter and ash content. The optimization process from the RSM showed that the most optimal value for torrefied OPEFB biochar were at 750 µm, 274°C and 90 minutes of torrefaction in order to produce a high energy content of biomass.

Kajian Pengoptimuman terhadap *Torrefied Biochar* dari Tandan Buah Kelapa Sawit Kosong (OPEFB) yang Berpotensi sebagai Tenaga Biomass

ABSTRAK

Permintaan dari seluruh dunia untuk tenaga dan penggunaan tenaga meningkat dengan pesat. Sumber biomas telah dipilih sebagai sumber tenaga yang boleh diperbaharui kerana terdapat banyak sisa kelapa sawit dihasilkan setiap bulan. Tujuan kajian ini dijalankan adalah untuk mencari nilai optimum proses pembakaran pada *torrefied biochar* daripada tandan buah kelapa sawit kosong (OPEFB) bagi menghasilkan sumber tenaga biomas dengan menggunakan reka bentuk Box-Behnken melalui kaedah gerak balas permukaan (RSM). Dalam kajian ini, OPEFB telah dibakar berdasarkan tiga pembolehubah bersandar yang bergantung kepada saiz partikel pada 250-750µm, suhu pebakaran pada 200-300°C, dan masa tinggal pada 30-90 minit. Proses pengoptimuman *torrefied biochar* adalah berdasarkan enam pembolehubah bebas yang merupakan hasil jisim, nilai kalori, karbon tetap, kandungan lembapan, bahan yang mudah meluap dan kandungan abu. Berdasarkan proses pengoptimuman, keputusan kajian menunjukkan bahawa nilai optimum bagi *torrefied biochar* OPEFB adalah pada partikel saiz 750 µm, pada suhu 274°C dan pada 90 minit masa tinggal bagi menghasilkan biomas yang mengandungi kandungan tenaga yang tinggi.

TABLE OF CONTENTS

LIST OF TABLES

LIST OF FIGURES

LIST OF ABBREVIATIONS

EFB	Empty fruit bunch
OPT	Oil palm trunk
PKS	Palm kernel shell
OPF	Oil palm fronds
FFB	Fresh fruit bunch
OPEFB	Oil palm empty fruit bunch
RSM	Response surface methodology
BP	British Petrol
M_Y	Mass yield
MC	Moisture content
VM	Volatile matter
AC	Ash content
FC	Fixed carbon
CV	Calorific value
H_2O	Water
CO_2	Carbon dioxide
SO_2	Sulphur dioxide
SO_3	Sulphur trioxide
N_2	Nitrogen
GHG	Greenhouse gaseous
RE	Renewable energy

BBD	Box-Behnken design
Mtoe	Million Tonnes of Oil Equivalent
MW	Megawatt
TWh	Terrawatt-hour
GWh	Gigawatt-hour
KWh	Kilowatt-hour

LIST OF SYMBOLS

%	Percentage
°C	Temperature (degree celcius)
>	Greater than
<	Less than
μm	Micrometer
Kg	Kilogram
Cm	Centimeter
MJ/kg	Megajoules per Kilogram

CHAPTER 1

INTRODUCTION

1.1 Background of Study

Energy demand and consumption are growing due to increasing population numbers. Renewable energy, which is the alternative energy, becomes really necessary to be used to offset the use of non-renewable fossil fuel energy, which is already hurting the atmosphere and the issues are getting worse due to climate change (Huang *et al*., 2017). More carbon dioxide is emitted to the atmosphere because of the industrial revolution and the combustion of fossil fuel. Climate change increase the global temperature, hence causing global warming and the world getting warmer. Human consumptions of energy and electricity keep increasing and thus more fossil fuel is needed as the source of energy.

Biomass is an alternative energy that generated from the biodegradable organic materials that undergo decomposition of plants and animals. Energy of biomass is derived from the interaction between plants and the sunlight, also known as photosynthesis. Biomass is an energy that sustainably produced to reduce the consumption of fossil fuel. This energy is able to derive about 44% from biomass that mostly based on wood and wood-derived materials. Biomass production in Malaysia is about 168 million tonnes such as oil palm waste, municipal waste and rice husks every single year (Salman, 2017). Renewable energy sources from the palm oil mill in Malaysia is rich in energy by utilizing the oil palm waste such as empty fruit bunch (EFB), oil palm trunk (OPT) and palm kernel shell (PKS). They act as a fuel by generating steam in the process of generating power by the movement of turbines (Abdullah *et al.*, 2013). The abundance of biomass that derived from the oil palm waste is able to cover the issue of generating a sustainable energy sources. Hence, the alternative energy will contribute in reducing the issue of global warming which is one of the solutions towards green energy production.

1.2 Problem Statement

Global energy consumption is the cumulative energy used by the entire human population. The total energy consumption is accelerating about +2.3% in 2017 compared to 1.1% in 2016 (Ranganadham, 2018). When time passes, the pattern in energy consumption will be increasing.

Malaysia is the second largest producer of palm oil after Indonesia. Thus, during the harvesting and extraction of oil palm fresh fruit bunch (FFB), oil palm mills produced abundance of oil palm waste. To find an alternative way to replace fossil fuel, oil palm waste biomass was seen as an alternative renewable energy that can generate energy from biomass. The oil palm waste such as oil palm empty fruit bunch (OPEFB) is able to replicate the ability of fossil fuel in generate energy by undergo the process of torrefaction, at the same time able to reduce the issues of climate change and global warming.

Currently, the Malaysian government is focused on replacing 5.5 percent of the electricity source with renewable energy as the country moves towards becoming a developed country by 2020 (Abas *et al.*, 2011). Based on the 2010 Malaysian Renewable Energy Act that was submitted to Parliament for approval in accordance with the Sustainable Energy Development Authority (SEDA) Act, the study focused on to promote the role of biomass as part of the Malaysia energy mix strategy.

Hence, the optimization of torrefied OPEFB as biochar energy is needed through optimizing the chosen parameters which are particle sizes, holding temperature and residence time. Torrefaction is suitable in improving the biomass' properties for the biomass energy generation.

1.3 Objectives

The objectives of this study are as follows:

a) To analyse torrefied OPEFB biochar using response surface methodology (RSM), Box-Behnken design according to OPEFB particle size, holding temperature and residence time of torrefaction process.
b) To identify the optimized torrefied OPEFB biochar regards to six responses of mass yield, calorific value, fixed carbon, moisture content, volatile matter and ash content.

1.4 Scope Of Study

The research is going to be conducted to identify whether the torrefied OPEFB biochar has a potential to be a biomass energy sources. Three dependent variables which are particle size, holding temperature and residence time will be involve in torrefaction process to synthesis the elements. The heating process of torrefied materials will be analyzed using the Box-Behnken design of response surface methodology. RSM will suggest the most optimum value based on the three parameters from the factors chosen. The method used became an approximation of functional relationship over all the responses of independent variables.

CHAPTER 2

LITERATURE REVIEW

2.1 Energy Overview

Energy is important since it is a basic need for a country's development. Communities are relying on the source of energy for daily routine. Malaysia's major generating plants are based on the hydropower and thermal power plant in generating electricity that comes from the primary energy sources.

Energy is classified into two energy sources that are renewable and non-renewable. Renewable energy is a source of energy that can be harvested from the non-depleting indigenous resources (Act 275, 2016). Meanwhile, non-renewable energy is the sources that cannot be replenish in thousands and million years, and will running out eventually. Fossil fuels are the most non-renewable sources that are consumed around the world for energy generation. Both of the sources are able to generate energy in order to fulfill the world energy demand. However, non-renewable energy sources will be facing depletion and gives negative impacts to the environment since non-renewable energy is limited and not a clean energy resource.

Currently, the main energy source is thermal power plant acts by converting the primary energy sources from fossil fuel such as coal to electricity. Thermal power plant has contributed about 119 TWh out of 134 GWh electricity generated for both power plant in Malaysia and the rest is hydro power plant (Samsudin *et* *al*., 2016). Fossil fuels which are coal, natural gas and coke contribute the most energy supply to Malaysia but the natural resources of fossil fuels are non-renewable. It happened that the sources are facing rapid depletion.

2.1.1 Energy Crisis and Energy Demand

Energy crisis is a global scenario that happened due to the demand and consumption. Energy is really important sources to country's economy growth. In order to meet the household worldwide energy demand, energy production going to be accelerate by 2050. Hence, the resources mainly fossil fuels are going to face depletion rapidly since the energy requirements from different sectors are depending on the fossil fuel energy generation (Eusoff, 2018).

The primary energy demand is based on the population, economy and also technology that used in supplying the energy to the different sectors. ExxonMobile (2018) reported that from 2010 to 2040, the global energy demand will be increasing about 35 percent. It shows that the growing population and economy contributed to the increasing of energy generation and production. Natural gas and coal will be the most demand sources of fossil fuel for power generation. However, the negative impact of the non-renewable energy becomes a concern due to the arising of pollution and greenhouse gases (GHG).

Based on the report by Statistics (2018) that shown at Figure 2.1, electric generation by fuel and plant in Malaysia is increasing. On 1992, about 30,000 GWh of electricity generated while in 2015, about 150,000 GWh of electricity generated which means that there is much higher compared to 1992. The results show the rapid acceleration of electricity that being generated. Hence, most of the energy sources that used to generate the electricity are fossil fuels mainly gas and coal. The burning of coal started to accelerate starting on 2004 until 2015 and will be accelerated if non-renewable energy source is the only option to generate electricity.

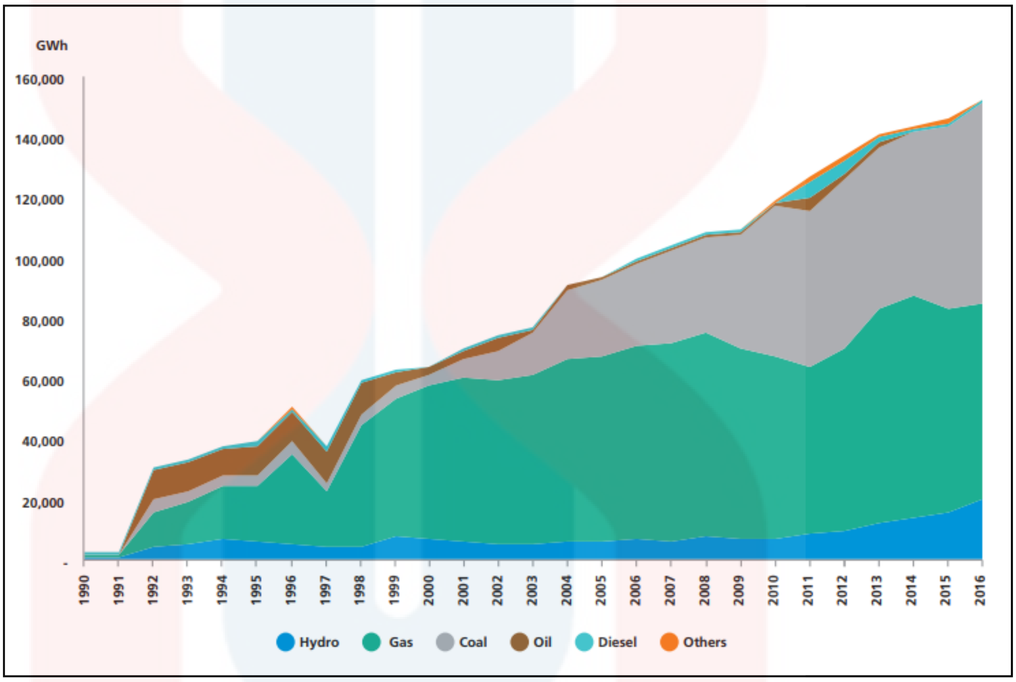

Figure 2.1: Electricity generation by fuel and plant. Source: (Eurostat, 2017)

Fossil fuels are made of hydrocarbons that are formed by the animals and plants' remain. Fossil fuel is also called mineral fuels since it is based on the hydrocarbon and extracted from earth. Fossil fuel provided about 80 percent of world energy demand which are coal, natural gas and also crude oil (Denchak, 2018). Thus, fossil fuel is facing depletion since it is not a renewable energy. The fossil fuel reserves left worldwide is also decreasing. Figure 2.2 shows the remaining fossil fuel available mainly coal, natural gas and oil before run out.

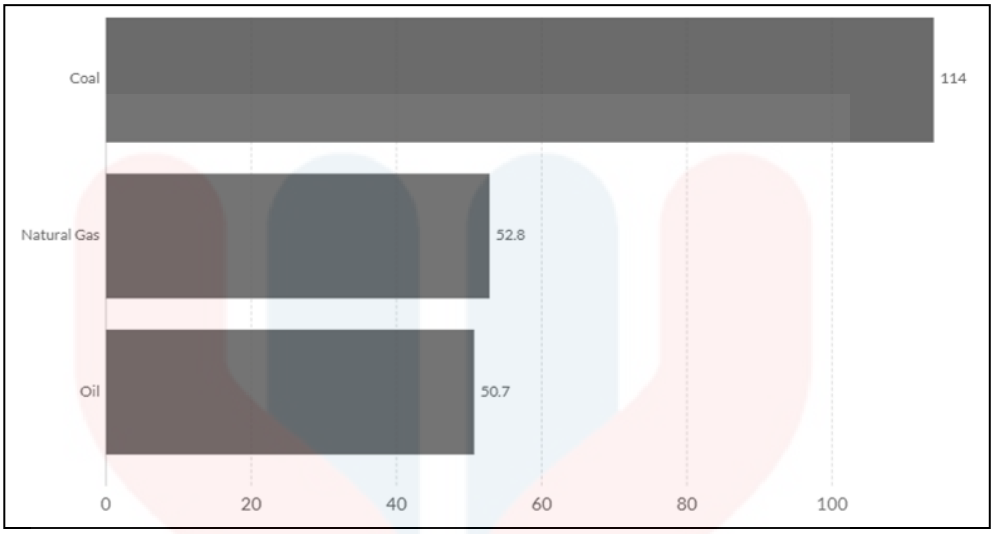

Figure 2.2: Years of fossil fuel reserves left (Source: BP, 2016)

Energy crisis in Malaysia happened due to the supply of fuel, market price and also energy security. It is because of the energy efficiency of non-renewable energy compared to renewable energy become an option for choosing non-renewable energy as the main energy generation in Malaysia. However, it becomes a concern by Malaysia based on National Energy Policy to secure the sources of energy for continuous of energy supply at the affordable price due to the depletion of fossil fuel which are coal, natural gas and crude oil (Tan, 2018). The sources of non-renewable energy are running out and even getting deplete eventually if the consumption of non-renewable energy sources are increasing every year. Table 2.1 shows the energy production analysis in Malaysia for 20 years from 2005 to 2030. The data shows that the energy production in Malaysia will be increasing almost seven times more than 2005. It is proven that Malaysia is relies on the fossil fuel which is the non-renewable energy as a sources of energy generation compared to renewable energy which is hydro. Only small portion of energy production that contributed by renewable energy source.

Table 2.1: Energy production analysis in Malaysia, 2005-2030

Fuel by Type	Electricity Production (GWh)		
	2005	2010	2030
Coal	23,134	49,675	154,686
Natural gas	55,899	55,700	139,025
Oil	2,489	2,855	3,107
Hydro	5,784	11,245	18,166
Total	87,306	119,475	315,984

(Source: Ministry of Energy, 2017)

2.1.2 Energy Consumption

Energy is important for human wellbeing. Energy is being consumed to generate electricity and for fuels. Nowadays, energy consumptions are increasing due to the economic growth and also population growth that contributed to the increasing of energy demand since energy is a basic foundation of a country's socio economic development. Figure 2.3 shows the world energy consumption by 2017. The data shows that the energy consumption is increasing rapidly. Besides, most of the energy sources being consume are originated from fossil fuel which are coal, natural gas and also crude oil.

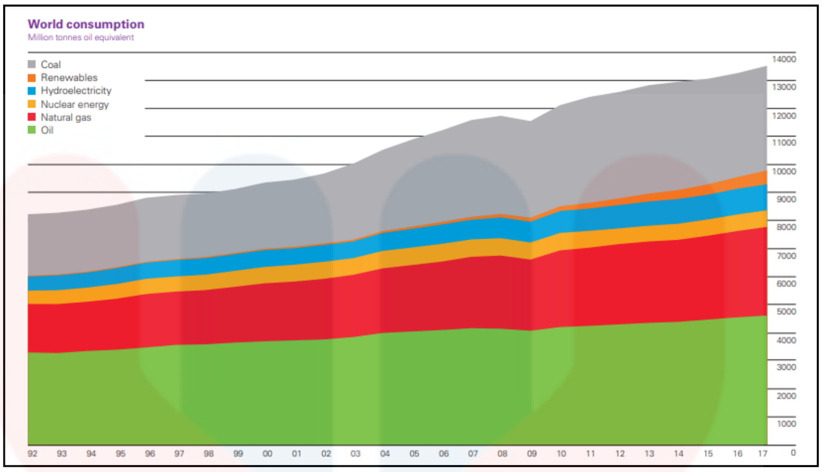

Figure 2.3: World energy consumption by 2017 (Source: BP, 2018)

Meanwhile, Figure 2.4 shows that the energy that being consumed based on the sectors and related to the economic and population growth. In 2015, the transportation is the biggest consumers of energy followed by industrial activities. Transportation consumed energy in form of fuel which is focused on oil and gas. The data show that energy consumption is increasing ten times in 2015 compared to 2,500 ktoe in 1980. It can be conclude that the population and economic growth contribute to the growing number of energy consumption in each sector.

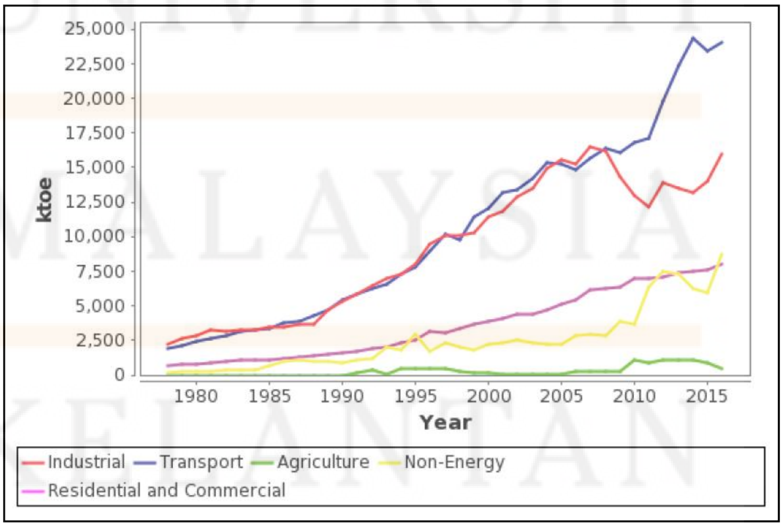

Figure 2.4: Energy that consumed based on the sectors

2.2 Renewable Energy

Renewable energy is a source of energy that comes from any resources that can be replenished by natural process on a human period and timescale. The rapid usage of renewable energy and energy efficiency giving benefits resulting in climate change mitigation, economic benefits and the energy security (Suhaimi *et al.*, 2013). Replacing non-renewable energy with renewable energy is one of the biggest mitigation options taken (Verbruggen *et al.*, 2010). In 1981, the four-fuel strategy has been adopted by Malaysian government that focused on having security supply of energy based on the national depletion policy in order to make sure the security of the energy supply. However, Malaysia's energy development towards renewable energy development is slow because lack of commitment and participation by the government. Currently, renewable energy is becoming much efficient and the growth in renewable energy production could end the consumption of fossil fuel.

The renewable energy (RE) field is a new alternative ways that is discovered by researchers and industrialist. The government have took part in nurturing sustainable development in Malaysia that focus on the RE topic. Malaysia also use renewable energy for energy generation which are hydro, biomass and solar. Renewable energy used to generate energy by harnessing sources from the nature such as heating and electricity. However, renewable energy is least option due some barriers such as to lack of knowledge and technology to harness the energy (Bayar, 2011). Table 2.2 shows the land resource requirement in order to produce 1 billion kWh/year of electricity.

Table 2.2: Land resource requirement to produce 1 billion kWh/year of electricity

Electrical Energy Technology	Land required (ha)
Hydroelectric power	75,000
Biomass	200,000
Wind power	9500
Photovoltaic	2800
Nuclear	30

(Source: Shafie *et al.*, 2011)

Despite the problems, renewable energy still chosen as sources of energy since there is significant reduction of pollutant of GHG that able to reduce global warming since carbon dioxide emitted by the fossil fuel is the biggest polluters that causing global warming and climate change. Hence, it reliable energy sources to generate energy compared to non-renewable energy such as fossil fuels (Suhaimi *et al.*, 2013). Malaysia also established renewable energy as fifth fuel in new Five Fuel Strategy in Eighth Malaysia Plan. RE also contribute to electric demand in Malaysia. Table 2.3 shows the potential energy resource, in ringgit value. It is because renewable energy sources have its value in ringgit. Thus, it helps to solve the global environmental issues and able to generate income for the country from the process of conversion of biomass into energy due to the abundance and continuous supply of biomass.

Table 2.3: Potential renewable energy resource, in ringgit

Renewable Energy Sources	Energy Value in RM Million (Annual)
Forest residues	11,984
Palm oil biomass	6,379
Solar thermal	3,023
Mill residues	836
Hydro	506
Solar PV	378
Municipal waste	190
Rice husk	77
Landfill gas	4

(Source: Goleman *et al.*, 2019)

2.3 Biomass

Biomass is a renewable energy resource that derived from the carbonaceous waste of either from human or natural activities. It can be from the by-products of agricultural crops or from the household waste. Biomass is mostly a plant based material that once derived from living organisms (Cho, 2016). Biomass is said to be renewable energy sources because the waste produced are abundance and always exist such forest resources and mill residues (Kamimoto, 2006).

Biomass is classified as a renewable and sustainable energy resource because the formation of biomass is originated from the interaction between carbon dioxide (CO_2), soil, sunlight, water and air with the presence of animals and plants. Microorganisms will break down the biomass after the living organisms are dead by producing water (H_2O), CO_2, and also potential energy (Shinn, 2018). The CO_2 produces are due to the process of microorganism degradation and combustion activities. Hence, the biomass combustion will be not increasing the total of CO_2 in the atmosphere that also known as *greenhouse neutral* or *GHG neutral*. Biomass is not categorized as a fossil fuel since it does not include any organic materials that are over millions of years. Table 2.4 shows the major groups of biomass and their classification.

Table 2.4: Two major groups of biomass and their sub-classification

Virgin biomass	1. Terrestrial biomass	i. Forest biomass ii. Grasses iii. Energy crops iv. Cultivated crops
	2. Aquatic biomass	i. Algae ii. Water plant
Waste biomass	1. Municipal waste	i. Municipal solid waste ii. Bio-solids, sewage iii. Landfill gas
	2. Agriculture solid waste	i. Livestock and manures ii. Agriculture crop residue
	3. Forestry residues	i. Bark, leaves, floor residues
	4. Industrial wastes	i. Demolition wood, sawdust ii. Waste oil/fat

(Source: Basu, 2013)

Biomass power is generated from the organic waste in order to reduce the waste that goes to the landfill or being burned. Energy form from the biomass by the heat released when the biomass is burned. Heat produced will form steam that will run the turbine to generate electricity. Energy from biomass also can reduce the carbon emission compared to fossil fuel that emits high carbon into the atmosphere, hence able to be a pollution control. Biomass was the oldest energy sources will able to be a substitute to the non-renewable energy of fossil fuel, thus, reducing the carbon which is greenhouse gases emission and impact to the environment (Ribeiro *et al.*, 2018). The abundance of biomass supply is able to secure the sources of energy supply for biomass energy production.

2.4 Biomass of Oil Palm Plantation

Oil palm plantation is the biggest agriculture activity in Malaysia and Malaysia is the second largest palm oil exporter in the world after Indonesia. Malaysia produced about 21.8 million tonnes of oil palm annually and the number keeps growing every year. It leads to huge production of oil palm biomass which happened became an environmental concern in disposing the waste properly (Drahansky *et al.*, 2016). Biomass produced from the palm oil industry is divided into two which are from the plantation activities such as pruning and replanting activities that generate trunks and fronds. Next is waste generated from the oil palm mills that processing the FFB for oil extraction and produced mesocarp fiber and OPEFB (Faizi *et al*., 2017).

However, the oil palm mills lead to the environmental degradation due to the development of mill itself and wastes generated after the oil extraction of fresh fruit bunches (FFB). Lots of water and energy sources are being used in processing the palm oil into products. There are several wastes produced from the oil palm mills such as mesocarp fruit fibers (MF), palm kernel shells (PKS) and empty fruit bunches (EFB) (Drahansky *et al.*, 2016). Meanwhile, the disposal of EFB without proper treatment lead to oil spills and burning EFB waste is wasting the renewable energy sources which able to be reused in boiler of palm oil mill (Abdullah *et al*., 2013).

The oil palm waste is sustainable and alternative way in disposing the waste and also able to generate energy due to the continuous supply, availability and the capacity. Thus, palm oil industry is really useful as the source of energy production. The sources are not relying on the palm oil products but the amount of by-products produced every single day. They were called them as bio-energy. Biomass produced from the waste generated from the fresh fruit bunch extraction will be used for palm oil mill operators to fuel the boilers as the energy sources. There are about 70% of fresh fruit bunch (FFB) that becoming a waste at the end of the extraction process (Zafar, 2018).

2.5 Biomass from Oil Palm Empty Fruit Bunch (OPEFB)

Empty fruit bunches (EFB) are the by-product or waste generated after the process oil pressing. EFB is rich with organic matter and nutrients. Oil palm empty fruit bunch (OPEFB) also has high saturated of water because of the steam sterilization at the mill. Moisture content in the EFB is about 67% and it needs to be dried before be considered as a source of biomass fuel. The raw EFB is very wet and in fibrous condition about 10 to 20cm length (Abdullah *et al.*, 2011). OPEFB can be produces into fuel by converting the EFB into pellets or bales after being processed. EFB is a sort of sustainable energy source since it is renewable energy, hence, give lots of benefit in sort of energy for the palm oil mill itself.

2.6 Torrefaction

Torrefaction is a thermochemical process in the environment that is inert or have limited oxygen available. The biomass is heated slowly in a specific range of temperature and maintain in there in specific time that gives result of near complete of degradation process of the hemicellulose content in order to achieve maximum mass and energy yield of the solid product (Basu, 2013).

Torrefaction is also a mild pyrolysis which the range of temperature for torrefaction process is between 200°C to 320°C. Temperature that more than the range will be resulting in an extensive devolatilization and carbonization of the polymers within the materials (Gronnow *et al*., 2013). Torrefaction is focus on sufficiently slow torrefaction rate to let maximization of solid yield. Torrefaction process is able to improve the quality of fuels for the application of combustion by changing the biomass properties. Torrefaction is always used to turn biomass into an energy source. The end products of torrefaction are always in form of fuel.

Torrefaction is a thermal process that is done by a contact with heat carrier. Figure 2.5 shows the products produced after the torrefaction reaction that generated from biomass fuel.

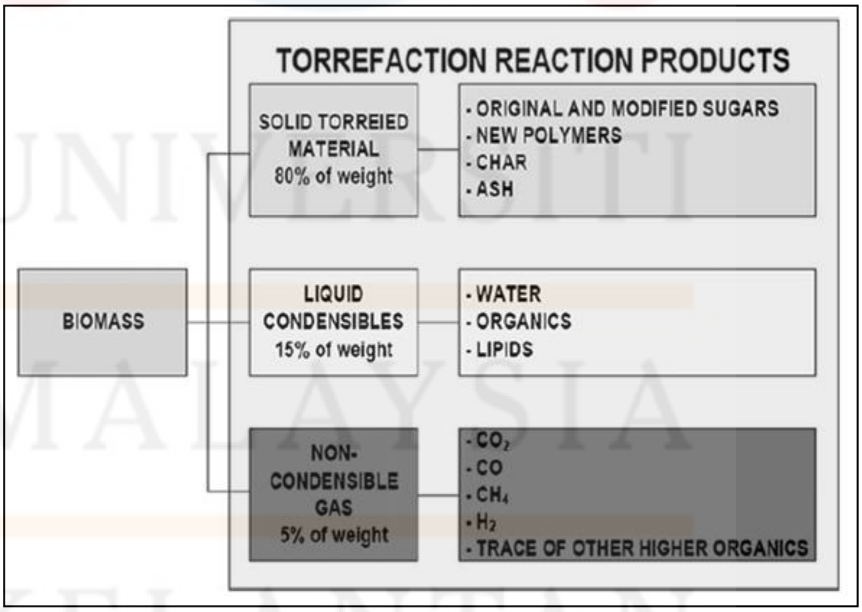

Figure 2.5: Products formed during the torrefaction process (Acharya *et al*., 2012)

The samples will be undergoes dry torrefaction that involves heating by inserting hot inert gas such as nitrogen gas which is an indirect heating. The heating process undergo in an inert environment because inert gases does not affect or alter the sample properties (Saadon *et al*., 2014). Commercial torrefaction usually chose dry torrefaction instead of wet torrefaction to reduce the moisture content.

2.7 Response Surface Methodology (RSM)

Response surface methodology (RSM) is a tool that was being introduced by Box and Wilson in early 1950s. RSM is a group of statistical and mathematical techniques that is being used in developing a process (Senaras, 2019). The application is focus on the designs and model for new products in order to improve the current products which act as the interest response that are being influenced by objectives and variables in order to optimize the responses (Myers, 2009). The extensive applications of RSM influence the performance measure of the process or product that called response. The subjects of the control of input variables are called independent variables.

Response surface are being represent in graphical form in order to help in visualizing the shape of response surface. The relationship between the response and the independent variables are unknown (Yin *et al*., 2008). An effective design of model parameter can be collected if proper experimental designs are used in data analysis. The actual objective of RSM was to determine which operating conditions that are optimum for the design experiment (Montgomery, 2009). RSM is also able to identify the operating requirements of factor space to be satisfied in order to achieve an extensive presentation of results.

2.7.1 Design of Experiment

Design of experiment (DoE) was designed and developed for the physical experiments of a model fitting. DoE was developed in order evaluated selection of responses since most of the DoE are made of a mathematical model which is an unknown structure of polynomials (Islam *et al.*, 2012). The design of experiments are differ each particular problems depend on the experimental design. Each different design gives a large difference on the approximation accuracy and the structure of response surface.

2.7.2 Box-Behnken Design (BBD)

Box-Behnken designs have much fewer design points compared to other design such as Central Composite Design. Box-Behnken design is much efficient and less expensive to be run with the identical number or amount of factors. It is able to estimate the first and second order coefficient. There are at least three levels for each factor and also minimum of three central points in each design. This model also designed to never include runs all of the factors at the extreme setting.

This type of response surface design is not being embedded to factorial or factorial design. Box-Behnken design contributes to the midpoints of the low and high factors combinations (Ferreira *et al*., 2007). It was designed to has at least three continuous factors that include the combination of midpoint of the experimental' edges. Box-Behnken design is a design which able to maintain the safe operating zone for the entire process. The model does not have any axial points that will let the all points remain in the safe operating zone. Besides, it will control the factors not to be run at the high levels at the same time.

2.7.3 Multi Response Optimization

Multi response optimization is to determine multiple response surfaces which have a set of response variables needs to be optimized simultaneously (Taylor *et al.*, 2013). The multiple responses are able to be analysed by using the RSM that focused on find the optimal conditions of selected variables that consists of minimum and maximum responses (He et al., 2010).

Multi response optimization are usually refers to RSM to convert the several responses into a single response index in order to find the optimal value of the dependent variables. The multiple responses that designed into a single response index will able to maximize the overall desirability. Some also called as composite desirability which able to compute the desirability functions between several responses. Overall desirability usually takes into account the maximum and minimum responses that are chosen before data being analysed.

CHAPTER 3

MATERIALS AND METHODS

3.1 Materials

The materials that used in this study are oil palm empty fruit bunch (OPEFB) that is derived from oil palm wastes. The samples were collected from the nearby mill that is located at Kemahang Palm Oil Mill, Jeli. OPEFB is selected in this study because of the abundance of OPEFB in Malaysia and the potential of OPEFB as a renewable energy source. Figure 3.1 showed the raw OPEFB before getting process and torrefied.

Figure 3.1: Raw OPEFB fiber before being processed

3.2 Methods

This study was divided into three which are the sample preparation, torrefaction of OPEFB into torrefied biochar, optimization of samples which was the data analysis of OPEFB (Lin, 2015).

3.2.1 Sample Preparation

Raw OPEFB were washed using tap water to remove any oils and impurities that present on the samples. The clean samples were dried under direct sunlight to dry the samples for a day. Then, the samples were dried in the oven about 1 hour at 103°C ± 2°C to reduce the moisture content in the samples. Then, the dried OPEFB were grinded to get smaller particle size.

The sample were screened into three different sizes which are 250, 500 and 750µm as shown in Figure 3.3 in order to obtain desired particle size and to prevent the contamination of other materials except the raw OPEFB since it will affect the final analysis.

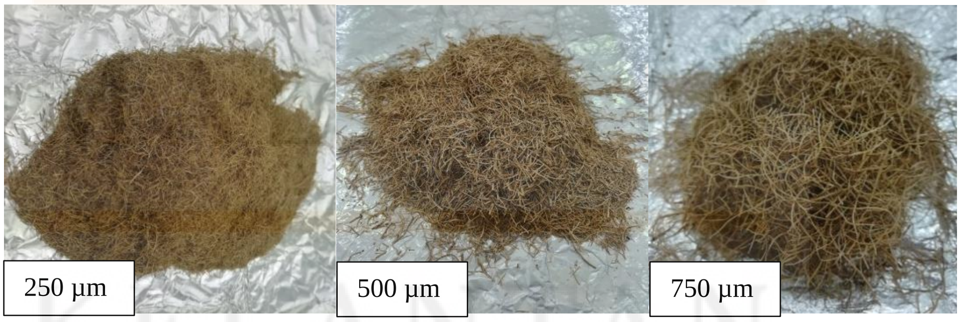

Figure 3.2: Screened OPEFB into three different sizes

3.2.2 Torrefaction Process

The OPEFB fibre was undergo torrefaction process which was the thermal pre-treatment method and being analyzed. The torrefaction process undergo three holding temperature which are 200°C, 250°C and 300°C without the presence of oxygen under slow heating rate (Zheng et al., 2017b). The samples were torrefied with three residence time which are 30, 60 and 90 minutes of torrefaction process (Huang *et al*., 2017). The raw materials of OPEFB are called torrefied OPEFB or biochar after the torrefaction process is complete.

3.2.3 Optimization

In order to get optimize data of torrefied' samples, a statistical technique which was response surface methodology (RSM) by using the Box-Behnken design was used in this study. This statistical technique was used to optimize the response that influenced by the independent variables which are the three parameters that used in this study (Senaras, 2019). The process of optimization by RSM analyzed the data based on six responses of independent variables which were mass yield, energy content (calorific value), fixed carbon, moisture content, volatile matter and ash content.

a) Mass yield

Mass yield was to measure solid yield that is remained in the materials after being torrefied. The mass yield was being calculated as shown in the Equation (3.1). Mass yield of the OPEFB was calculated by dividing the final weight that was the torrefied OPEFB by the initial weight that was the raw OPEFB and times by 100 percent.

$$Mass\ yield\ (\%) = \left(\frac{Final\ weight)}{(Initial\ weight}\right) \times 100\% \qquad (3.1)$$

b) Proximate analysis

Proximate analysis gave the composition of the torrefied biomass in the terms of gross components which were moisture content (MC), volatile matter (VM), ash content (AC) and fixed carbon (FC). This analysis was considered easy and cheap to be process (Omar *et al.*, 2017).

The gross composition of torrefied OPEFB was determined by running proximate analysis. There were four analysis which are moisture content (MC), volatile matter (VM), ash content (AC) and fixed carbon (FC).

i) Moisture Content

Moisture content of torrefied biochar analyzed the moisture content by using analyzer MX-50 according to ASTM D3173 standard. The sample was placed on the sample support and the reading will be reset to 0g. Then, the pan was placed with sample which not exceeding 3g. The sample was analyzed after the heating cap is closed and the data of MC shown when the signal rings. The MC of torrefied biochar was identified based on the Equation (3.2) shown.

$$MC\ (\%) = \frac{(Wi - Wf)}{Wf} \times 100 \qquad (3.2)$$

Where Wi = initial weight (g) and Wf = final weight (g)

ii) Volatile Matter

The analysis of volatile matter was analyzed by using the ASTM D3175 standard procedure. About 1g of torrefied biochar was placed in crucible without cap was weighed and recorded. Then, the samples were placed inside and burnt at 900°C for 7 minutes. Samples were weighed using analytical balance after being cool down. The VM is calculated by using Equation (3.3).

$$VM\ (\%) = \frac{(Wi - Wf)}{Wi} \times 100 \qquad (3.3)$$

Where Wi= initial weight (g) and Wf = final weight(g)

iii) Ash content

Ash content analysis was based on the standard procedure of ASTM D3174 by using the furnace heating. The crucible used for volatile matter analysis used without cap by heating in the furnace. The torrefied samples were weighed by analytical balance after being cool down. Ash content from torrefied materials were calculated based on Equation (3.4).

$$AC(\%) = \frac{Weight\ of\ ash}{Wr} \times 100 \qquad (3.4)$$

Where Wr=weight of residues (moisture free) (g)

iv) Fixed carbon

The fixed carbon (FC) was calculated by deducting percentage of moisture content, volatile matter and the ash content by 100% of each sample. Fixed carbon was calculated by using Equation (3.5).

$$FC\ (\%) = 100 - (MC(\%) + VM(\%) + AC(\%)) \qquad (3.5)$$

c) Energy content

Energy content or calorific value was the heat released from a unit mass of fuel after a complete combustion. Energy content was calculated by thermodynamic value and being expressed in kJ/kg. It usually determined by the calorimeter and theoretical value. The energy content test was really important in order to determine the effect of torrefection in increasing and improvising the energy content of the biomass.

Auto calorimeter 500 instrument also known as bomb calorimeter was used based on ASTM D2015 standard. The sample was weight more than 1g to be ideal in order to avoid invalid combustion. Together with a piece of cotton wool, sample was placed in the crucible. The sample was passed through a specified length of fuse wire with both ends of the wire attached to the 2 electrodes of the bomb. Ignition wire was set up by coiling the wire on the U-shape and connects it to the connector. Then, connect wire in the chamber to a bucket of distilled water. The calorimeter then closed by transfer the bomb head to the bomb containers, care must be taken not to damage the sample. The calorimeter then filled with oxygen supply and the chamber also was set to be in dry condition and the sample in holder crucible was placed at workstation before oxygen valve being opened. The bucket within bomb was filled and handled carefully. Once power source was connected, the stirrer was run and the data was recorded. The value of energy content of torrefied OPEFB was calculated based on Equation (3.6, 3.7 and 3.8).

$$Y_m = \frac{Weight\ of\ mass\ after\ torrefaction}{Mass\ of\ raw\ OPEFB} \tag{3.6}$$

$$CV_R = \frac{CV\ sample\ after\ torrefaction}{CV\ of\ raw\ OPEFB} \tag{3.7}$$

$$Ye = Y_m \times CV_R \tag{3.8}$$

Where CV_R : calorific value, Y_m : mass loss, and Ye: energy content

3.3 Data Analysis

Using the RSM, which was the Box-Behnken design based on the three parameters that were particle size, holding temperature and residence time for variable energy content, sample optimization was performed. The response of data that recorded was analyzed via regression. Data optimization was run by using MINITAB 15 and Design Expert 7 software.

3.3.1 Normal Probability Plot and Histogram

Response surface design software was designed to provide four type of analysis which was normal probability plot, histogram, versus fit and versus order. Normal probability and histogram plot were chosen since both of them are the significant residual plot for this study.

3.3.2 Regression Analysis

Regression analysis was made based on the estimated regression coefficients for each six responses. The estimated regression coefficient provided p-value for each factors based on 95 percent desirable confident level that was chosen for this study. P-value that showed < .050 is the most significant factors while > .050 was insignificant factor on the results of the study.

3.3.3 Equation of Regression Analysis

The optimum value of the responses was based on the Equation (3.9) in order to prove the optimal value for each of the responses. The data were retrieved from the p-value provided by the estimated regression coefficients.

$$y = mx + c \tag{3.9}$$

3.3.4 Contour Plot and Surface Plot

The contour plot display the 3 dimensional relationship of mass yield, holding temperature and residence time in 2 dimensional graphs. Contour and surface plot were design based on each responses and factors that gave significant impacts on the result. Two of three factors were chose as the x-axis and z-axis to see the correlation between each of the responses in 3 dimensional graph in order to estimate the optimal value based on the center points that was suggested by the plot.

3.3.5 Multi Response Surface

This method was describing the multiple response surface aspect on RSM technique based on several responses that were analyzed into one type of composite desirability.

Table 3.1: Desirable goal of response optimizer

Parameter	Goal
Mass yield	Maximum
Calorific value	Maximum
Fixed carbon	Maximum
Moisture content	Minimum
Volatile matter	Minimum
Ash content	Minimum

All the six responses were set based on desirable goal listed in Table 3.1. OPEFB must have a high mass yield, calorific value, fixed carbon and low moisture content, volatile matter and ash content in order to produce high-quality biomass energy sources. Thus, maximum and minimum goals were chose based on desirable target.

CHAPTER 4

RESULTS AND DISCUSSION

4.1 Mass Yield

The mass yield of the OPEFB showed decreasing value from the initial weight compared to the final weight after being torrefied. The initial weights were approximately 5.00g for all 17 times run. The final weight of OPEFB after torrefaction process showed that the mass loss up to 68%. The final mass yields were calculated based on formula of Equation (3.1) stated in Chapter 3. Mass yield represent the percent ratio of the actual ratio of OPEFB mass (Helmenstine, 2019). The higher the mass yield, the higher the energy sources in the OPEFB samples. Lowest mass yield was 31.95% while the highest mass yield 97.86%.

Due to the high concentration of volatile composition in feed EFB, high mass reduction occurs on the basis of mass yield obtained. High mass loss also occurs during drying periods, where high levels of moisture are decreased before being put in the torrefaction reactor. In order to obtain most desirable energy source, the mass yield of the torrefied OPEFB biochar was targeted to be maximum (Awang *et al.*, 2019).

The critical point found from the result of this study was nearing a minimum point. However, it was desired to obtain reaction conditions within the ranges that could produce biochar with maximum mass yield (Md Arshad *et al.*, 2019).

4.1.1 Normal Probability Plot

Based on the Figure 4.1, the data plotted against theoretical normal distribution were mostly on the normal line. Only the first and last points are outliers that are isolated from the other from the normal line. The data plot shows a long tails which the curve starts below the normal line and followed by a bend.

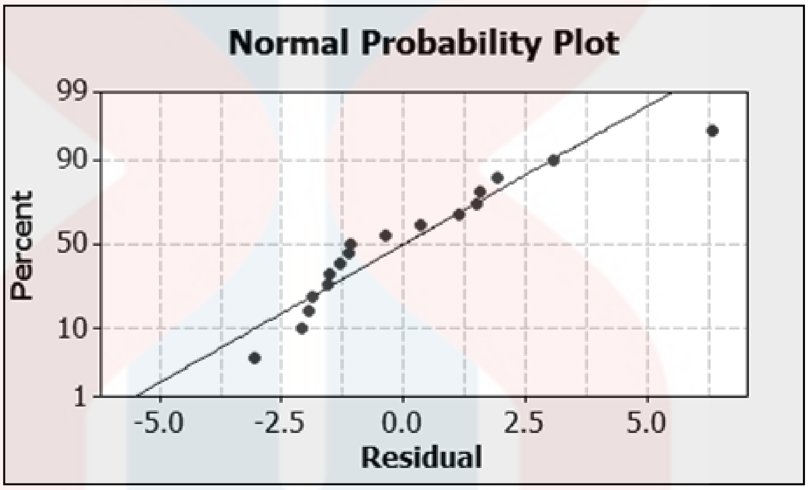

Figure 4.1: Normal probability plot of mass yield

4.1.2 Histogram

The following graph based on Figure 4.2 was a right-skewed on one side of the histogram. It shows that the sample data were biased to the left of the histogram graph. Right skewed graph shows that the mean comes to the right of the mode (Muniz, 2017). Meanwhile, there was an outlier also called as gap which was located at the left side of the graph showed that the variables are discrete (Lesik, 2010).

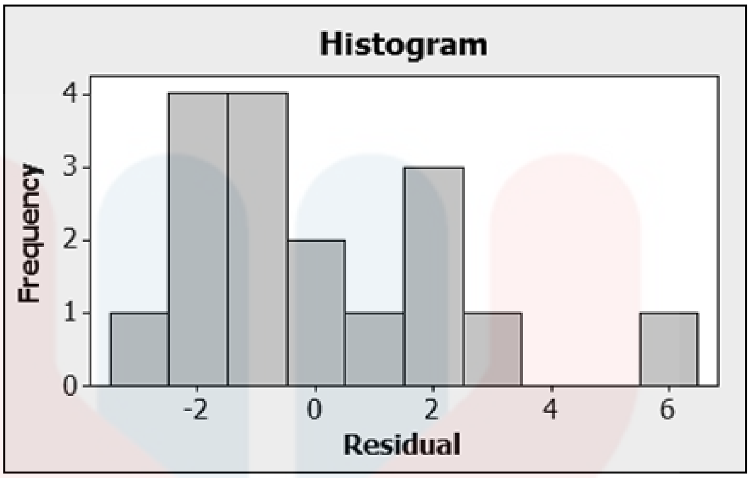

Figure 4.2: Histogram plot of mass yield

The mass yield mode was the highest histogram peak which was -2 and -1, whereas the average was 1.7 calculated from the average frequency. The histogram's median was 8.5 which fell in the -1 residual.

4.1.3 Regression Analysis

P-value signifies the relationship of the results based on the statistical test (McLeod, 2019). Regression coefficients analysis based on Figure 4.3 proved that some of the p-value of mass yield was not statistically significant to the research hypothesis.

Estimated Regression Coefficients for Mass Yield

Term	Coef	SE Coef	T	P
Constant	-143.903	50.9223	-2.826	0.026
Particle Size	0.023	0.0479	0.484	0.643
Holding Temperature	2.298	0.3642	6.311	0.000
Residence Time	0.421	0.3989	1.056	0.326
Particle Size*Particle Size	-0.000	0.0000	-1.053	0.327
Holding Temperature* Holding Temperature	-0.005	0.0007	-7.832	0.000
Residence Time*Residence Time	0.001	0.0019	0.440	0.673
Particle Size*Holding Temperature	0.000	0.0001	0.286	0.783
Particle Size*Residence Time	-0.000	0.0002	-0.130	0.900
Holding Temperature*Residence Time	-0.003	0.0012	-2.440	0.045

Figure 4.3: Estimated regression coefficients of mass yield

Particle size (A) and residence time (C) did not give a statistically significant value of 0.643 and 0.326 which was much higher than 0.050. It proved that the results of the experiment did not relate to the variables of particle size and residence time. Meanwhile, p-value of holding temperature (C) is 0.000 which was very significant to the experiment.

4.1.4 Regression Analysis Equation of Mass Yield

As the findings' novelty, the value of y was calculated on the basis of Chapter 3's equation (3.9). The y-value of mass yield was the optimum response value based on the estimated mass yield regression coefficient.

$$y = mx + c$$

$$y = 0.643A + 0B + 0.326C + 0.327A^2 + 0B^2 + 0.673C^2 + 0.783AB + 0.900AC + 0.045BC + 0.026$$

Where A: particle size, B: holding temperature, and C: residence time

4.1.5 Contour Plot

The particle size was the most insignificant factor based on the regression analysis and became a hold value of 500 µm which was the medium value of the in the graph.

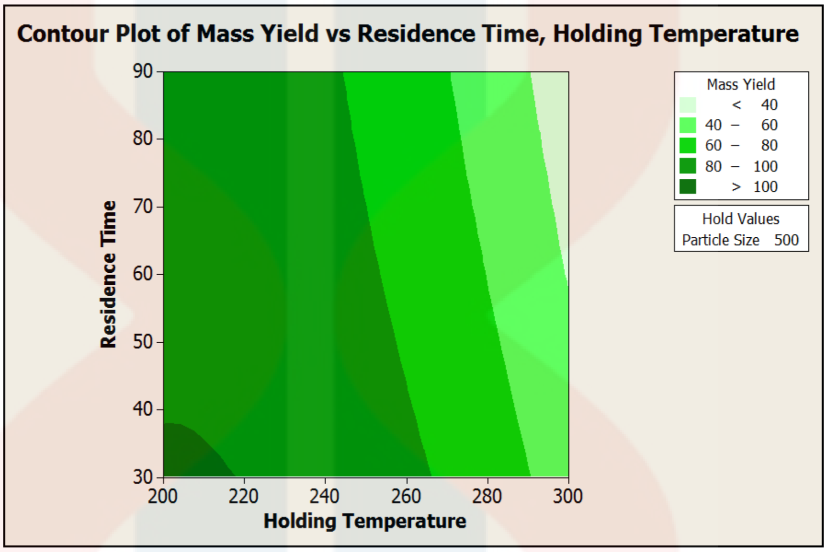

Figure 4.4: Contour plot of mass yield vs residence time and holding temperature

Based on contour plot in Figure 4.4, the mass yield was approximately 100% from 200-220°C. As the temperature increase, from 220-265°C the mass yield was gradually decreased to 80% and constantly decreased to 40% when temperature reached 290°C. Meanwhile, residence time showed slightly changes at 30-40 minutes which was 100% mass yield. As the time increased, there was no significant change on the mass yield. It can be concluded that holding temperature gave a significant impact to the mass yield compared to residence time.

4.1.6 Surface Plot (3D Graph)

The surface contour in Figure 4.5 acts almost the same to the contour plot. Due to the not significant results of the mass yield, particle size was chosen as hold value of 500 µm. The red point at the centre of surface plot indicates the optimal value of mass yield.

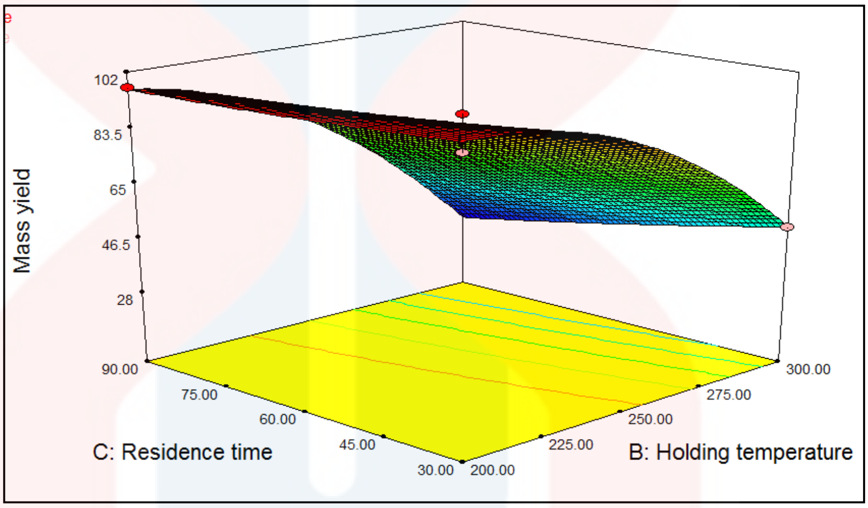

Figure 4.5: Surface plot of mass yield

Based on the surface plot, it can be estimated that the optimal value of mass yield was 65% when the residence time at 60 minutes and holding temperature at 250°C. Holding temperature gave a significant changes on mass yield compared to the residence time.

4.2 Calorific Value

The calorific value is the amount of heat generated during the combustion process. It can also measure the torrefied biochar's heating capacity by estimating the amount of biochar needed to produce a certain amount of heat. A higher calorific value in char indicates the higher energy content in the char. Recent studies showed that the impact of torrefaction on the OPEFB gradually reduced the calorific value of the biomass (Pulka *et al.*, 2019). The research therefore aimed at obtaining the highest calorific value to produce high-quality OPEFB biochar by taking all the parameters into account and achieving the optimum energy content value.

4.2.1 Normal Probability Plot

Based on the Figure 4.6, most of the data plotted against normal theoretical distribution was on the normal line. It showed that a normal data distribution. Only the first point was outlier, far from the normal line and isolated from the others. The data plot revealed a short tail that begins far higher than the normal line with S-shaped curve and indicated a shorter tail than the normal distribution.

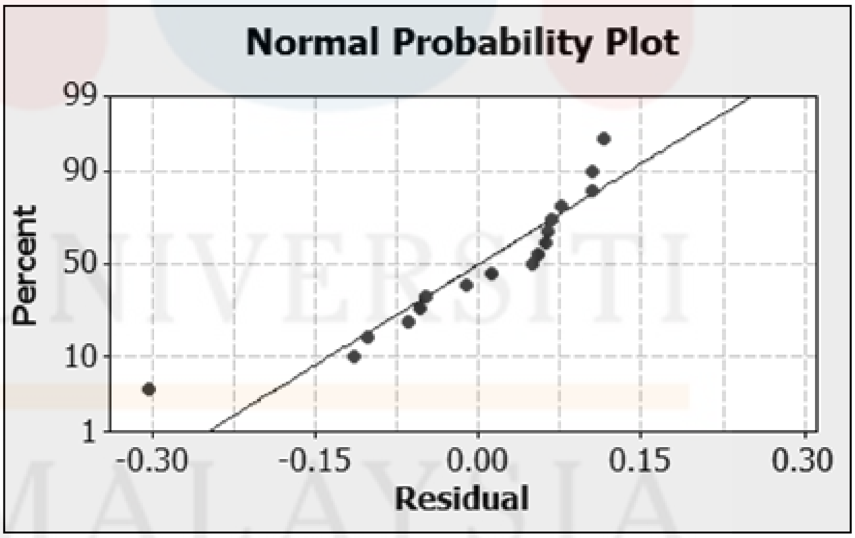

Figure 4.6: Normal probability plot of calorific value

4.2.2 Histogram

The following graph based on Figure 4.7 was located on one side of the histogram which was a left-skewed. It showed that the sample data were biased to the right of the histogram graph. Left skewed graph showed that mean came to the left of the mode. Meanwhile, there was an outlier also called as gap which was located at the left side of the graph showed that the variables are discrete.

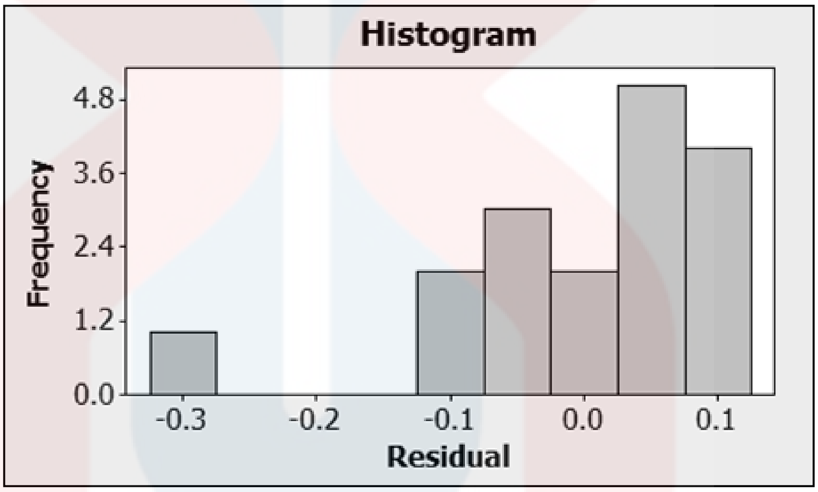

Figure 4.7: Histogram plot of calorific value

The mode of the calorific value was the highest peak of the histogram which was 0.05, while the mean was 2.8 that calculated from the average frequency. The median of the histogram was falls in group 0.05.

4.2.3 Regression Analysis

Analysis of the regression coefficients based on Figure 4.8 showed that the p-value of calorific value was statistically significant to the hypothesis of the study.

Estimated Regression Coefficients for Calorific Value

Term	Coef	SE Coef	T	P
Constant	25.7207	2.31261	11.122	0.000
Particle Size	-0.0074	0.00217	-3.401	0.011
Holding Temperature	-0.0554	0.01654	-3.347	0.012
Residence Time	-0.0343	0.01812	-1.896	0.100
Particle Size*Particle Size	0.0000	0.00000	1.338	0.223
Holding Temperature* Holding Temperature	0.0001	0.00003	3.290	0.013
Residence Time*Residence Time	0.0002	0.00009	1.894	0.100
Particle Size*Holding Temperature	0.0000	0.00001	3.265	0.014
Particle Size*Residence Time	0.0000	0.00001	0.270	0.795
Holding Temperature*Residence Time	0.0001	0.00005	1.516	0.173

Figure 4.8: Estimated regression coefficients for calorific value

Residence time (C) gave the value of 0.100 which fell just short of a statistical significant that was higher than 0.05 was not statistically significant. It proved that there was no relationship between the variables of residence time on the results of the experiment.

Meanwhile, p-value of particle size (A) and holding temperature (B) is 0.011 and 0.012 which was very significant to the experiment.

4.2.4 Regression Analysis Equation of Calorific Value

The value of y as the novelty of the results was determined on the basis of Chapter 3's Equation (3.9). The y-value of calorific value represented the optimal value of the response based on the estimated regression coefficient of calorific value.

$$y = mx + c$$

$$y = 0.011A + 0.012B + 0.100C + 0.223A^2 + 0.013B^2 + 0.100C^2 + 0.014AB + 0.795AC + 0.173BC + 0$$

Where A: particle size, B: holding temperature, and C: residence time

4.2.5 Contour Plot

The particle size was the most negligible factor based on the regression analysis and became a hold value of 500 µm, which was the variable medium value in the graph. Dark to lighter colour indicated the increase of response.

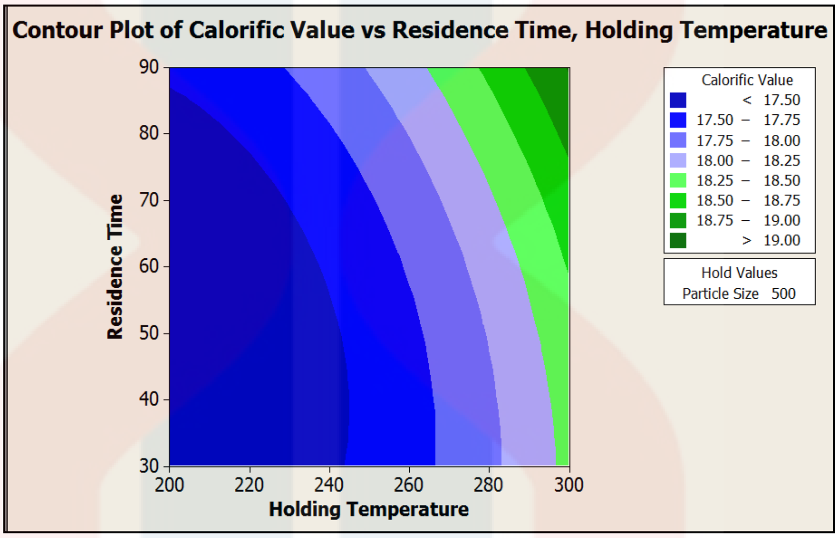

Figure 4.9: Contour plot of calorific value vs residence time and holding temperature

Depending on the contour plot in Figure 4.9, the holding temperature gave the calorific value significant changes as the temperature rose. From 200°C the calorific value was the least which was lower than 17.50 MJ/kg but slowly increased as the temperature increased to 240°C. Starting on 265°C to 295°C, the calorific value gradually increased and reached the highest calorific value which was higher than 19.00 MJ/kg at 300°C.

Meanwhile, residence time did not show any significant changes on the calorific value. From 30-85 minutes the calorific value was remained the same and slightly increased to 17.50 MJ/kg at 85 minutes. It can be concluded that the changes of holding temperature gave a significant impacts on the calorific value relative to the residence time.

4.2.6 Surface Plot (3D Graph)

The surface contour in Figure 4.10 acts nearly the same as the contour plot. Due to the insignificant calorific value results, particle size was chosen as hold value of 500 µm.

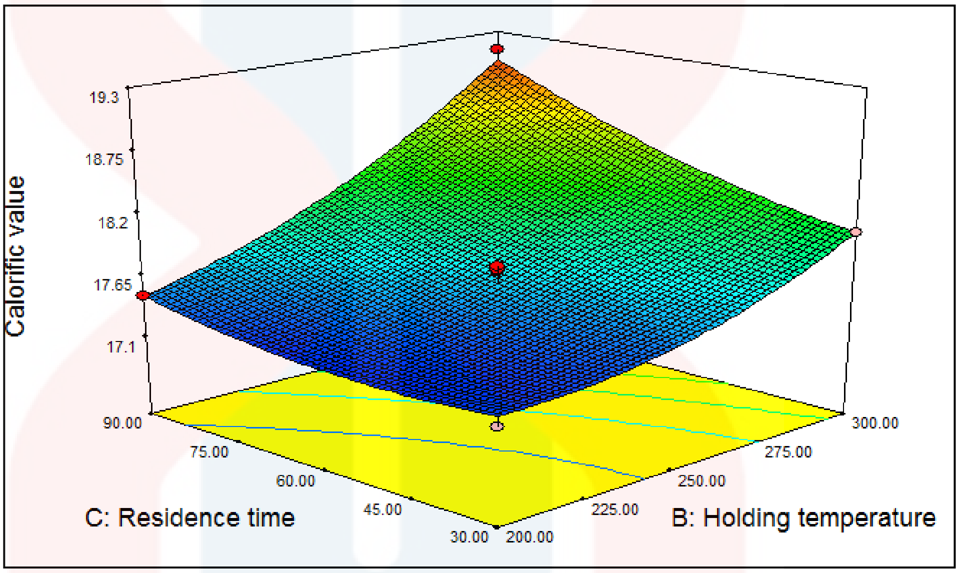

Figure 4.10: Surface plot of calorific value

In the centre of the surface graph, the red point showed the optimum calorific value. Based on the surface plot, it can be estimated that the optimal value of calorific value was 17.65 MJ/kg when the residence time at 60 minutes and holding temperature at 250°C.

4.3 Fixed Carbon

Fixed carbon is a residue portion of the char after combustion processes, excluding the volatile, humidity and ash content (Speight, 2015). Fixed carbon was calculated on the basis of the other parameters measured in the proximate analysis.

4.3.1 Normal Probability Plot

The data plotted against normal theoretical distribution formed an approximately straight line based on the graph in Figure 4.11. It showed that the data distribution fit the normal line indicated that the fixed carbon data distribution was normal.

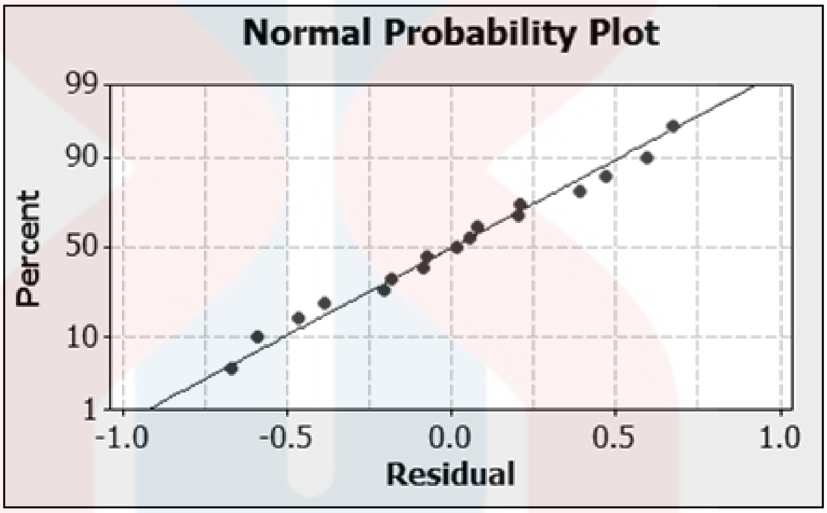

Figure 4.11: Normal probability plot of fixed carbon

4.3.2 Histogram

The graph in Figure 4.12 showed a normal distribution graph. It was a bell-shaped graph where clusters of information occur on one side of the average which occurs on the other side of the average as well. There was no gap between the bas that showed that the variables are continuous.

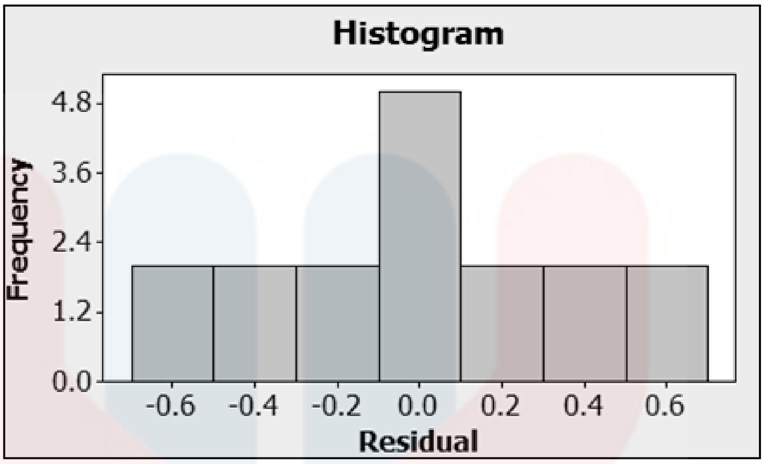

Figure 4.12: Histogram plot of fixed carbon

The mode of fixed carbon was located at the centre of the histogram which 0.0 residual values. Mean value of fixed carbon was 2.4 and the median was falls in group 0.

4.3.3 Regression Analysis

Regression coefficients analysis in Figure 4.13 proved that p-value of fixed carbon was statistically significant to the research hypothesis. Particle size (A) gave the value of 0.261 which was not significant to the independent variables that was much higher than 0.05 was not statistically significant. This showed that on the experiment's findings there was no interaction between the particle size variables.

Estimated Regression Coefficients for Fixed Carbon

Term	Coef	SE Coef	T	P
Constant	173.861	8.56820	20.291	0.000
Particle Size	-0.010	0.00805	-1.224	0.261
Holding Temperature	-1.553	0.06128	-25.349	0.000
Residence Time	-0.183	0.06712	-2.724	0.030
Particle Size*Particle Size	0.000	0.00000	3.414	0.011
Holding Temperature* Holding Temperature	0.004	0.00012	30.174	0.000
Residence Time*Residence Time	-0.001	0.00033	-2.301	0.055
Particle Size*Holding Temperature	-0.000	0.00002	-1.644	0.144
Particle Size*Residence Time	0.000	0.00004	2.200	0.064
Holding Temperature*Residence Time	0.001	0.00020	7.147	0.000

Figure 4.13: Estimated regression coefficients for fixed carbon

Meanwhile, p-value of holding temperature (B) and residence time (C) are 0.000 and 0.030 which was very significant to the experiment. Thus, they support the probability of research hypothesis to be true.

4.3.4 Regression Analysis Equation of Fixed Carbon

As the novelty of the findings, the value of y was calculated based on the Equation (3.9) from Chapter 3. Fixed carbon y-value represented the optimum response value based on the estimated fixed carbon regression coefficient.

$$y = mx + c$$

$$y = 0.261A + 0B + 0.030C + 0.011A^2 + 0B^2 + 0.055C^2 + 0.144AB + 0.064AC + 0BC + 0$$

Where A: particle size, B: holding temperature, and C: residence time

4.3.5 Contour Plot

Based on the regression analysis, particle size was the most insignificant factor and became a hold value which is 500 µm which was the medium value of the factor in the graph. Light to darker colour indicated the increase of response.

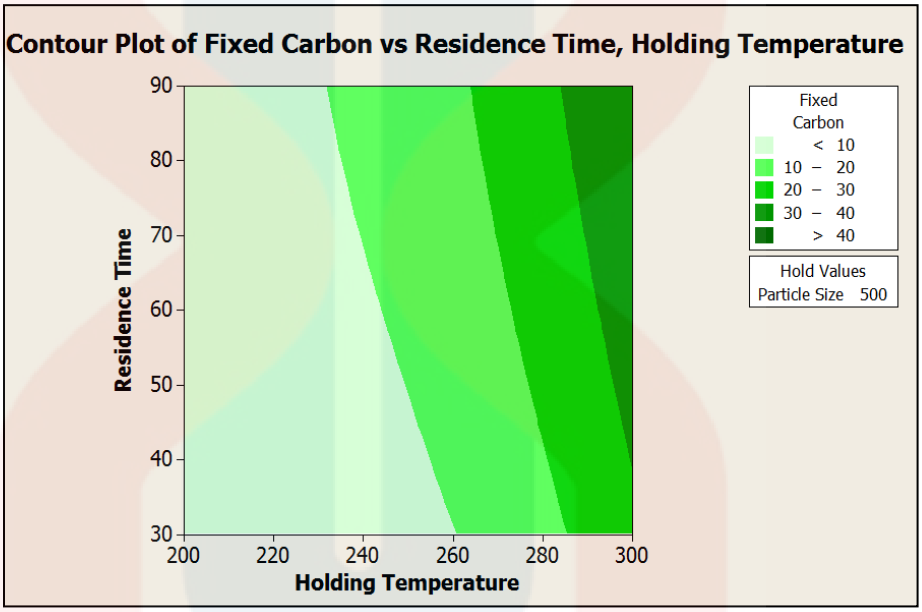

Figure 4.14: Contour plot of fixed carbon vs residence time and holding temperature

Based on contour plot in Figure 4.14, there was no significant change on the fixed carbon on the holding temperature from 200-260°C. The fixed carbon gradually increased starting on 260°C which the fixed carbon value increased to 10-20%. At 285°C there was visible change on the fixed carbon value which was about 20-30%.

In the meantime, there was no change in the residence time in the fixed carbon as the time increased. It can therefore be inferred that holding temperature has led to changes in fixed carbon while residence time has not been relevant to changes in fixed carbon value.

4.3.6 Surface Plot (3D Graph)

The surface contour plot in Figure 4.15 acts almost the same to the contour plot. Particle size was chose as hold value due to the not significant results of the fixed carbon.

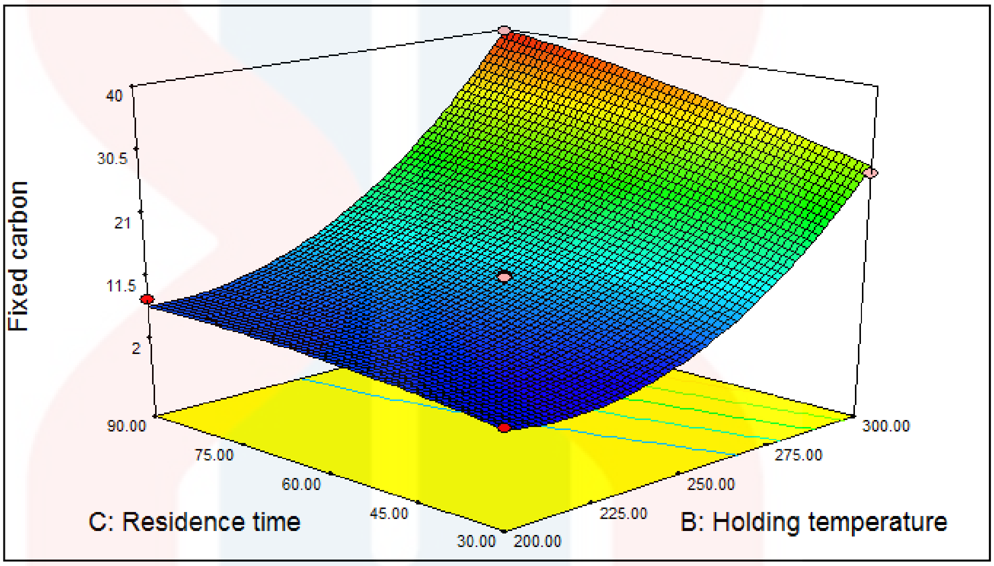

Figure 4.15: Surface plot of fixed carbon

In the middle of the surface graph, the red point represents the optimum value of fixed carbon. Based on the surface plot, it can be estimated that the optimal value of fixed carbon was 11.50% when the residence time at 60 minutes and holding temperature at 250°C.

4.4 Moisture Content

Moisture content is the total moisture in any form of water that resides in the biochar after being torrefied. Moisture content was measured from the mass of water lost from the sample under specific heating rate. The study focused on minimizing and reducing the moisture content and produce OPEFB biochar with higher calorific value (Karthikeyan, 2008). The elimination of water was an integral part of the process. Coal water content also has a significant effect on the coal's utilization. Reducing the moisture content of the torrefied OPEFB biochar added to the rise in the energy content calorific value.

4.4.1 Normal Probability Plot

The data plotted against normal theoretical distribution formed an approximately straight line based on the graph in Figure 4.16. It showed that the data distribution of fit the normal line showed that the moisture content distribution of the data was normal.

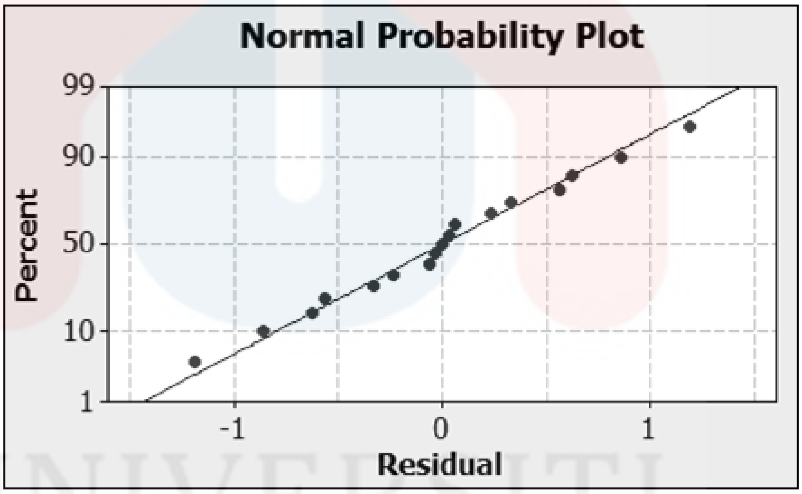

Figure 4.16: Normal probability plot of moisture content

4.4.2 Histogram

The graph in Figure 4.17 showed a normal distribution graph. It was a bell-shaped diagram which appears on one side of the average data samples that also occur on the other side of the average.

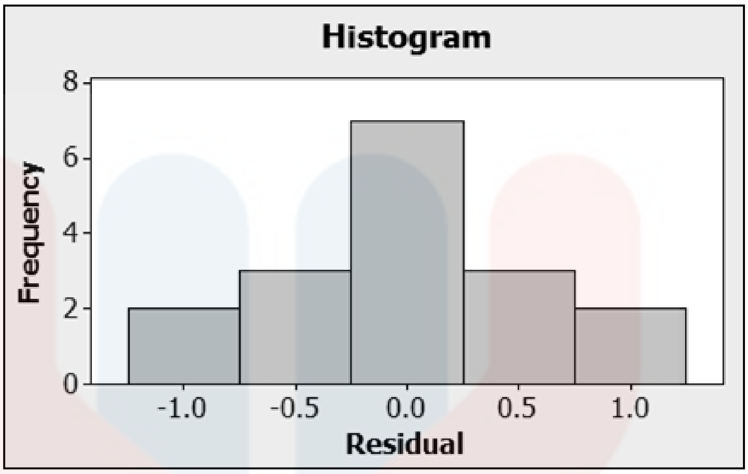

Figure 4.17: Histogram plot of moisture content

There was no gap between the bars showing continuity of the variables. The value of mode was shown at the centre of the histogram which 0.0 residual values. The mean of the histogram was 0 and the median was also 0.

4.4.3 Regression Analysis

Analysis of the regression coefficients in Figure 4.17 showed that the p-value of moisture content was not statistically relevant to the research hypothesis. All the dependent variables were not significant to the research hypothesis. Particle size (A) gave the value of 0.247, holding temperature (B) is 0.335 and residence time (C) was 0.291 which were very not significant to the independent variables.

Estimated Regression Coefficients for Moisture Content

Term	Coef	SE Coef	T	P
Constant	16.8840	13.2731	1.272	0.244
Particle Size	0.0158	0.0125	1.264	0.247
Holding Temperature	-0.0982	0.0949	-1.035	0.335
Residence Time	0.1186	0.1040	1.141	0.291
Particle Size*Particle Size	-0.0000	0.0000	-0.453	0.664
Holding Temperature* Holding Temperature	0.0002	0.0002	1.031	0.337
Residence Time*Residence Time	-0.0006	0.0005	-1.179	0.277
Particle Size*Holding Temperature	-0.0000	0.0000	-0.547	0.602
Particle Size*Residence Time	-0.0001	0.0001	-2.326	0.053
Holding Temperature*Residence Time	0.0000	0.0003	0.096	0.926

Figure 4.18: Estimated regression coefficients for moisture content

The p-value of moisture content was so much higher than 0.05 that was not statistically significant to the value of moisture content. It proved that there was no relationship on the results of the experiment between all the variables.

4.4.4 Regression Analysis Equation of Moisture Content

The value of y was determined as the novelty of the results based on the Chapter 3 Equation (3.9). The y-value of the moisture content was the optimal response value based on the estimated moisture level regression coefficient.

$$y = mx + c$$

$$y = 0.247A + 0.335B + 0.291C + 0.664A^2 + 0.337B^2 + 0.277C^2 + 0.602AB + 0.053AC + 0.926BC + 0.244$$

Where A: particle size, B: holding temperature, and C: residence time

4.4.5 Contour Plot

Based on the regression analysis, particle size is the most insignificant factor and becomes a hold value which is 500 μm which was the medium value of the factor in the graph. Light to darker colour indicates the increase of response. According on the contour plot in Figure 4.18, a significant change in moisture content depending on the contour plot was produced by both holding temperature and residence time.

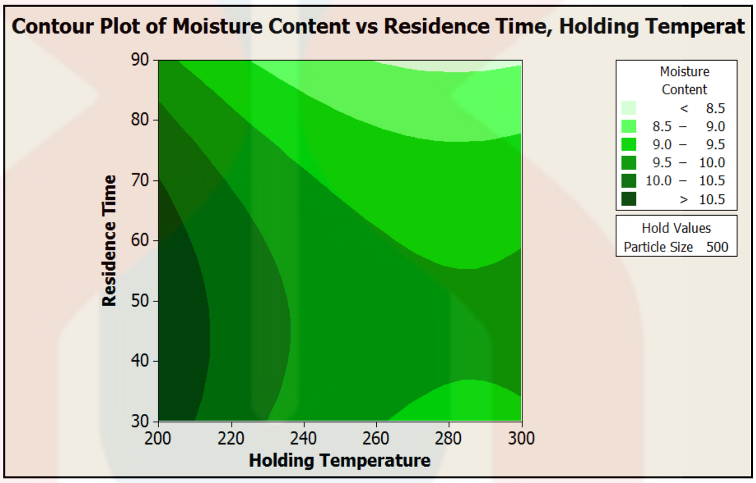

Figure 4.19: Contour plot of moisture content vs residence time and holding temperature

In order to produce high energy content of char, the study needed to achieve lowest value of moisture content. From 200°C to 260°C, there was significant change of moisture content. The moisture content was gradually decreased from 10.5% up to 8.5%.

Meanwhile, as the residence time increased there was slightly change of moisture content starting on 70 minutes to 80 minutes and the value gradually decreased. Based on the regression analysis, the moisture content was not significantly changed by all factors, but the contour plot showed a visible change in moisture content that obeyed the goal of reducing the moisture content value in the torrefied biochar.

4.4.6 Surface Plot (3D Graph)

The surface contour in Figure 4.19 acts almost the same to the contour plot. Particle size was chose as hold value due to the not significant results of the moisture content. The red point at the centre of surface plot indicates the optimal value of moisture content. Based on the surface plot, it can be estimated that the optimal value of moisture content was 9.65% when the residence time at 60 minutes and holding temperature at 250°C.

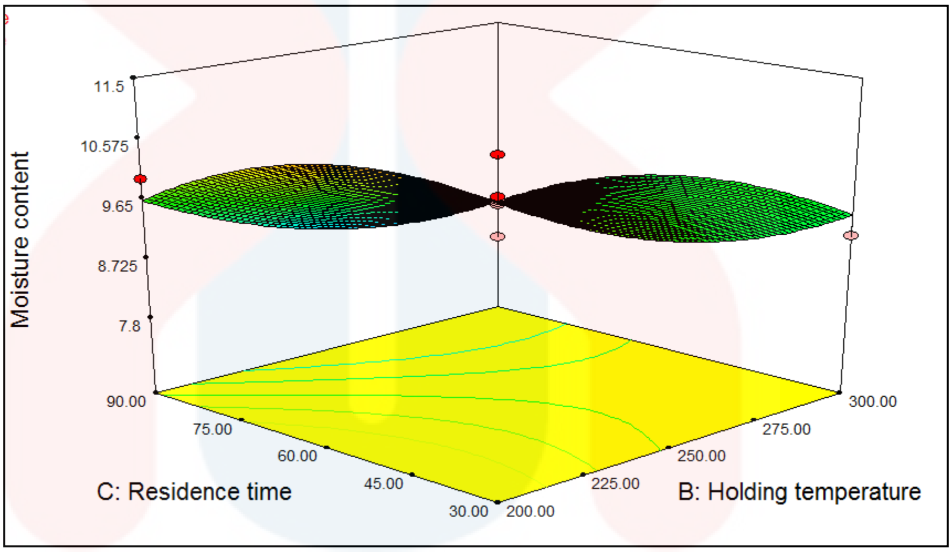

Figure 4.20: Surface plot of moisture content

4.5 Volatile Matter

Volatile matter was referring to the components of the biochar after being torrefied without the presence of oxygen excluding the moisture content. It was a measure of gases that formed during torrefection process. The higher temperature corresponded to a more intense reaction, resulting in more volatile generation that escaped mainly in the form of gas. Thus, the volatile matter was increased as the holding temperature and residence time of torrefaction increased. The analysis aimed at minimizing volatile matter and previous research showed that volatile matter increased but could be minimized by optimizing torrefaction factors (Zheng *et al.*, 2017).

4.5.1 Normal Probability Plot

Based on the graph in Figure 4.20, the data plotted against theoretical normal distribution formed an approximately a straight line. It showed that the distribution of volatile matter data fit the normal line indicated that the data distributions are normal.

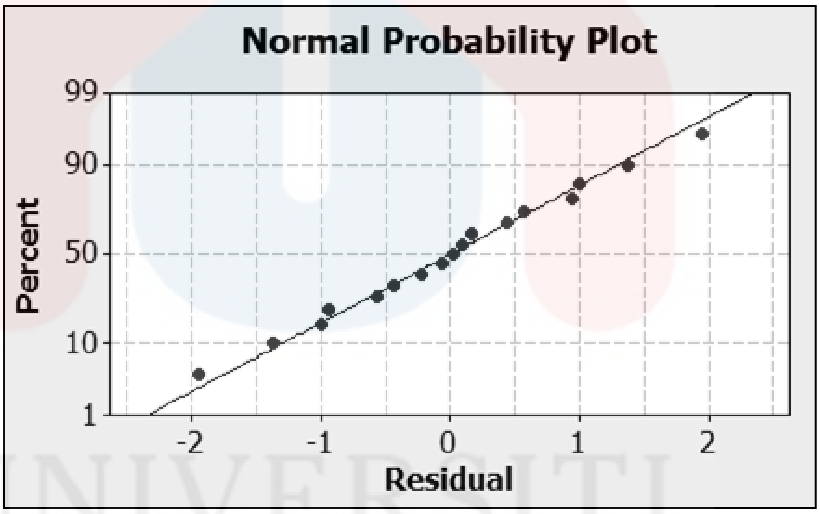

Figure 4.21: Normal probability plot of volatile matter

4.5.2 Histogram

The graph in Figure 4.21 showed a normal distribution graph. It was a bell-shaped graph which data samples occurred on one side of the average that also occurred to the other side of average.

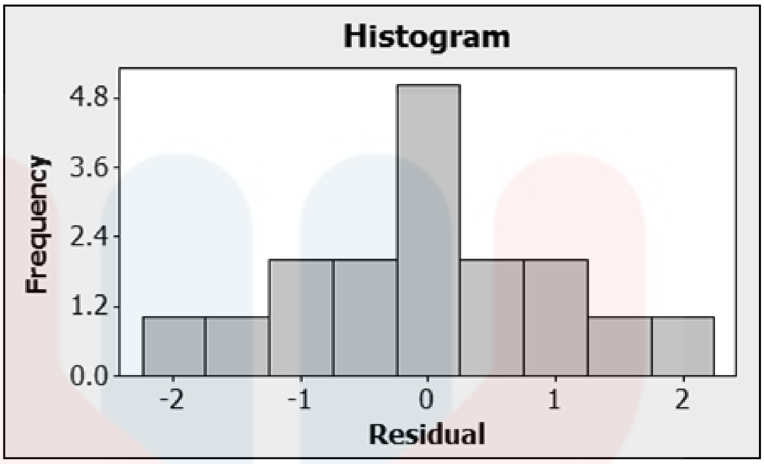

Figure 4.22: Histogram plot of volatile matter

There was no gap between the bas that showed that the variables were continuously. The mode was at the centre of the histogram which 0 residual values. The mean of the histogram was 0 and the median was also 0.

4.5.3 Regression Analysis

Regression coefficients analysis in Figure 4.22 proved that some of the p-value of volatile matter was not statistically significant to the research hypothesis. Particle size (A) and residence time (C) gave the value of 0.702 and 0.648 which were much higher than 0.05 is not statistically significant.

Estimated Regression Coefficients for Volatile Matter

Term	Coef	SE Coef	T	P
Constant	-109.072	21.6876	-5.029	0.002
Particle Size	-0.008	0.0204	-0.398	0.702
Holding Temperature	1.813	0.1551	11.689	0.000
Residence Time	0.081	0.1699	0.477	0.648
Particle Size*Particle Size	-0.000	0.0000	-1.396	0.205
Holding Temperature* Holding Temperature	-0.004	0.0003	-13.839	0.000
Residence Time*Residence Time	0.001	0.0008	1.801	0.115
Particle Size*Holding Temperature	0.000	0.0001	1.427	0.197
Particle Size*Residence Time	0.000	0.0001	0.653	0.535
Holding Temperature*Residence Time	-0.002	0.0005	-3.283	0.013

Figure 4.23: Estimated regression coefficients for volatile matter

It proved that there was no relationship between the variables of particle size and residence time on the results of the experiment. Meanwhile, p-value of holding temperature (C) is 0.000 which was very significant to the experiment.

4.5.4 Regression Analysis Equation of Volatile Matter

As the novelty of the findings, the value of y was calculated based on the Equation (3.9) from Chapter 3. The y-value of volatile matter represented the optimal value of the response based on the estimated regression coefficient of volatile matter.

$$y = mx + c$$

$$y = 0.702A + 0B + 0.648C + 0.205A^2 + 0B^2 + 0.115C^2 + 0.197AB + 0.535AC + 0.013BC + 0.00$$

Where A: particle size, B: holding temperature, and C: residence time

4.5.5 Contour Plot

Based on the regression analysis, particle size is the most insignificant factor and becomes a hold value which is 500 µm which was the medium value of the factor in the graph. Dark to lighter colour indicated the increase of response.

Based on contour plot in Figure 4.23, from 200-260°C, there was no significant change of volatile matter. From 260°C the value of volatile matter was decreasing to 70% and gradually decreased until 300°C. Meanwhile, residence time do not show any change in value of volatile matter. It can be concluded that residence time does not have a significant impact on the volatile matter and the holding temperature showed slight changes as the temperature rose.

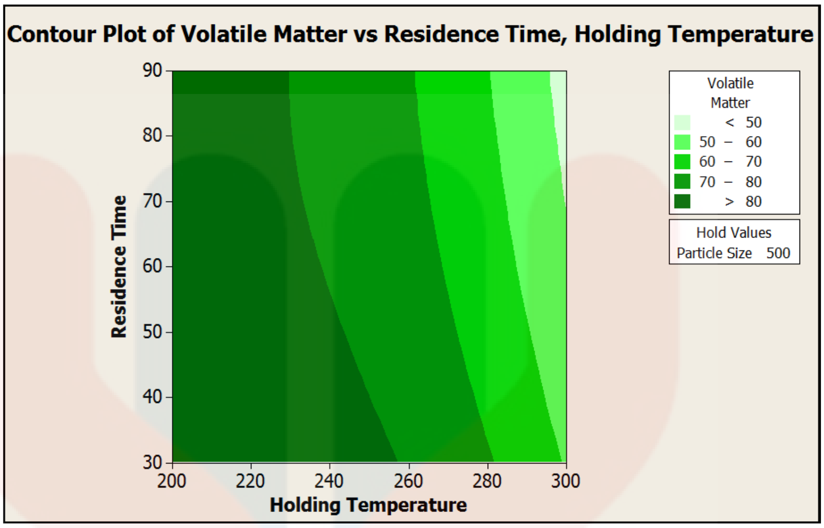

Figure 4.24: Contour plot of volatile matter vs residence time and holding temperature

4.5.6 Surface Plot (3D Graph)

The surface contour in Figure 4.24 acts almost the same to the contour plot. Particle size was chose as hold value due to the not significant results of the volatile matter. The red point at the centre of surface plot indicated the optimal value of volatile matter. Based on the surface plot, it can be estimated that the optimal value of volatile matter was 76% when the residence time at 60 minutes and holding temperature at 250°C.

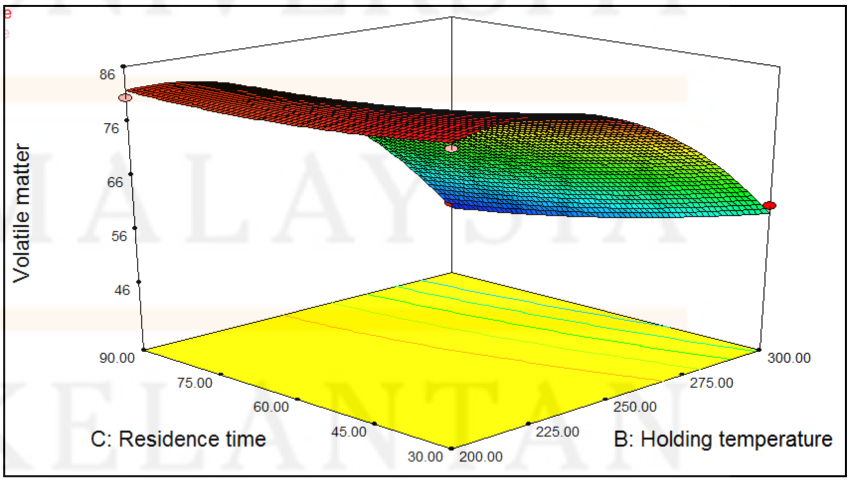

Figure 4.25: Surface plot of volatile matter

4.6 Ash Content

Ash content was a part of the torrefied biomass that was made of the incombustible mineral material. A large amount of ash content was not favour due to the potential released of ashes during the process of combustion (Tumuluru, 2015). The study showed that ash content in the measured biomass decreased as the holding temperature and torrefaction period rose. The increase in the composition of ash is more proportional to the shift of the original components of biomass. As the biomass loses some of the moisture and volatiles during the process, the ash content is more of a relative increase with respect to the original components.

4.6.1 Normal Probability Plot

Based on the graph in Figure 4.25, the data plotted against theoretical normal distribution formed an approximately a straight line. It showed that the distribution of data fit the normal line indicated that the data distributions of ash content were normal.

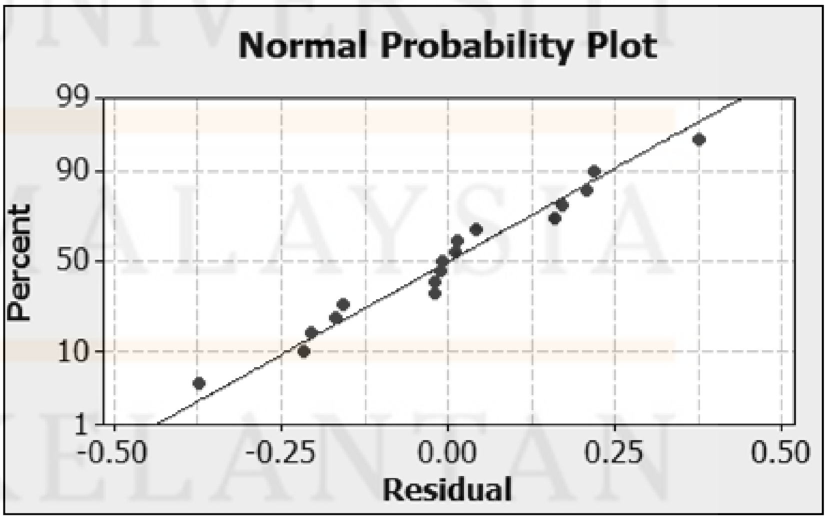

Figure 4.26: Normal probability plot of ash content

4.6.2 Histogram

The graft in Figure 4.26 showed a normal distribution graph. It was a bell-shaped graph which data samples occurred on one side of the average that also occurred to the other side of average.

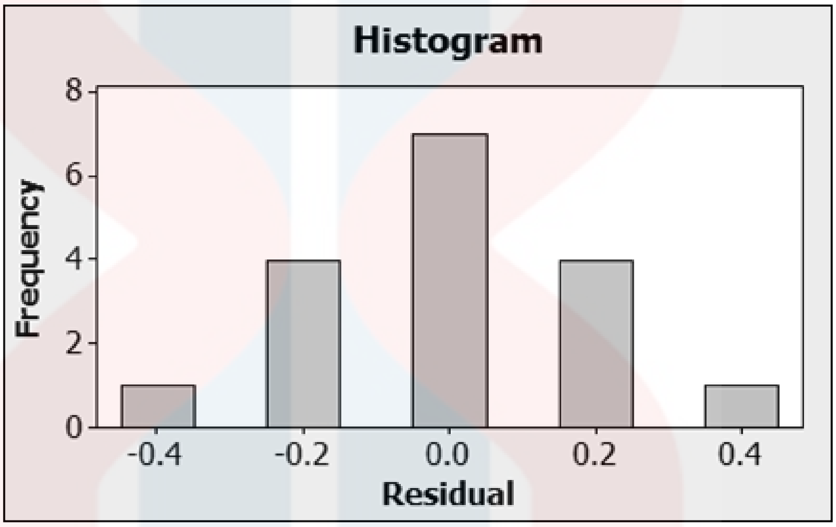

Figure 4.27: Histogram plot of ash content

However, the present of the gaps showed that the variables were discrete. The mode of the ash content was at the centre of the histogram which 0.0 residual values. The mean of the histogram was 0 and the median was also 0.

4.6.3 Regression Analysis

Regression coefficients analysis in Figure 4.27 proved that some of the p-value of ash content was not statistically significant to the research hypothesis. Particle size (A) and residence time (C) gave the value of 0.580 and 0.614 which were much higher than 0.05 is not statistically significant. It proved that there was no relationship between the variables of particle size and residence time on the results of the experiment.

Estimated Regression Coefficients for Ash Content

Term	Coef	SE Coef	T	P
Constant	18.3275	4.04639	4.529	0.003
Particle Size	0.0022	0.00380	0.580	0.580
Holding Temperature	-0.1614	0.02894	-5.578	0.001
Residence Time	-0.0168	0.03170	-0.528	0.614
Particle Size*Particle Size	0.0000	0.00000	1.740	0.125
Holding Temperature*Holding Temperature	0.0004	0.00006	6.898	0.000
Residence Time*Residence Time	-0.0001	0.00015	-0.911	0.393
Particle Size*Holding Temperature	-0.0000	0.00001	-2.373	0.049
Particle Size*Residence Time	-0.0000	0.00002	-0.527	0.614
Holding Temperature*Residence Time	0.0002	0.00009	2.145	0.069

Figure 4.28: Estimated regression coefficients for ash content

Meanwhile, p-value of holding temperature (C) is 0.001 which was very significant to the experiment. Thus, it supported the probability of research hypothesis to be true.

4.6.4 Regression Analysis Equation of Ash Content

As the novelty of the findings, the value of y was calculated based on the Equation (3.9) from Chapter 3. The y-value of ash content represented the optimal value of the response based on the estimated regression coefficient of ash content.

$$y = mx + c$$

$$y = 0.580A + 0.001B + 0.614C + 0.125A^2 + 0B^2 + 0.393C^2$$
$$+ 0.049AB + 0.614AC + 0.069BC + 0.003$$

Where A: particle size, B: holding temperature, and C: residence time

4.6.5 Contour Plot

Based on the regression analysis, particle size is the most insignificant factor and becomes a hold value which is 500 µm which was the medium value of the factor in the graph. Light to darker colour indicates the increase of response.

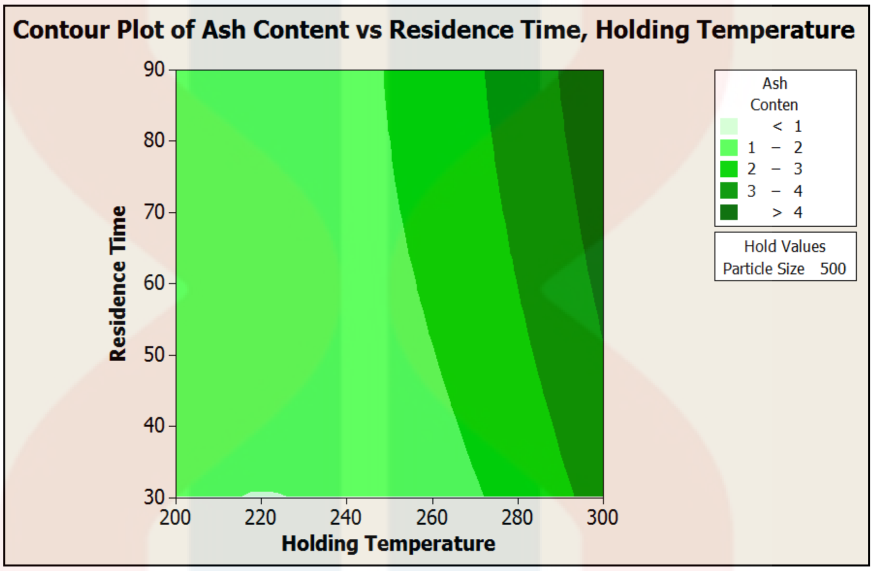

Figure 4.29: Contour plot of ash content vs residence time and holding temperature

Based on the contour plot in Figure 4.28, the value of ash content was remained at 200-270°C and gradually increased from 2-3% on 280°C. The value of ash content increased as the holding temperature reached 300°C into 3-4%. Meanwhile, residence times did not give any significant change on the value of ash content as the time increased. It can be concluded that holding temperature contributed to the change ash content value and residence time did not.

4.6.6 Surface Plot (3D Graph)

The surface contour in Figure 4.29 acts almost the same to the contour plot. Due to the insignificant results of the ash content, particle size was selected as hold value. In the centre of the surface graph, the red point showed the optimum ash content value.

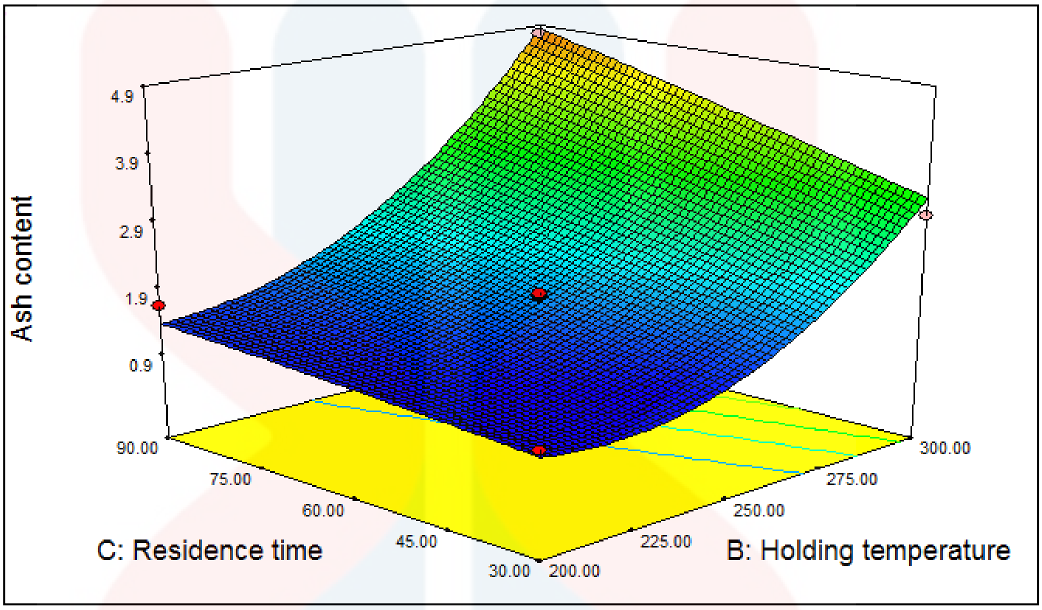

Figure 4.30: Surface plot of ash content

Based on the surface plot, it can be estimated that the optimal value of ash content was 1.90% when the residence time at 60 minutes and holding temperature at 250°C.

4.7 Multi Response Surface Analysis

By optimizing the problems, multiple RSM were able to give an analysis involving multiple factors and multiple responses. RSM was able to analyse a number of decision spaces as well as the factor levels that gave an optimal value to one.

4.7.1 Optimization Plot

The optimization plot of mass yield, calorific value, fixed carbon, moisture content, volatile matter and ash content was based on Figure 4.30. The plot showed the composite desirability that computes an optimal and presents them in a single optimization plot. Within the experimental range, three-dimensional surfaces were plotted to show the effect of each factor along with interaction effects between different factors

The red line will indicate the changes happened in each response in order to determine the way, how it can affect the responses and represent the current factor settings. The composite desirability was changed by moving the red line to achieve the highest composite desirability. The optimization plot showed the composite desirability was 0.62866 which was acceptable and valid in this study.

The y-value showed that the optimum value of mass yield was 55.58% at particle size 750 µm, holding temperature 274.12°C and residence time of 90 minutes. Particle size showed very small visible changes as the size increased and gave small change on the mass yield as the time increased. Holding temperature gave a significant change of mass yield as the temperature increased. The graph of temperature for mass yield showed negative slope. As the temperature increased, the value of mass yield decreased. Residence time also showed slightly negative slope. As the time increased, the mass yield also decreased.

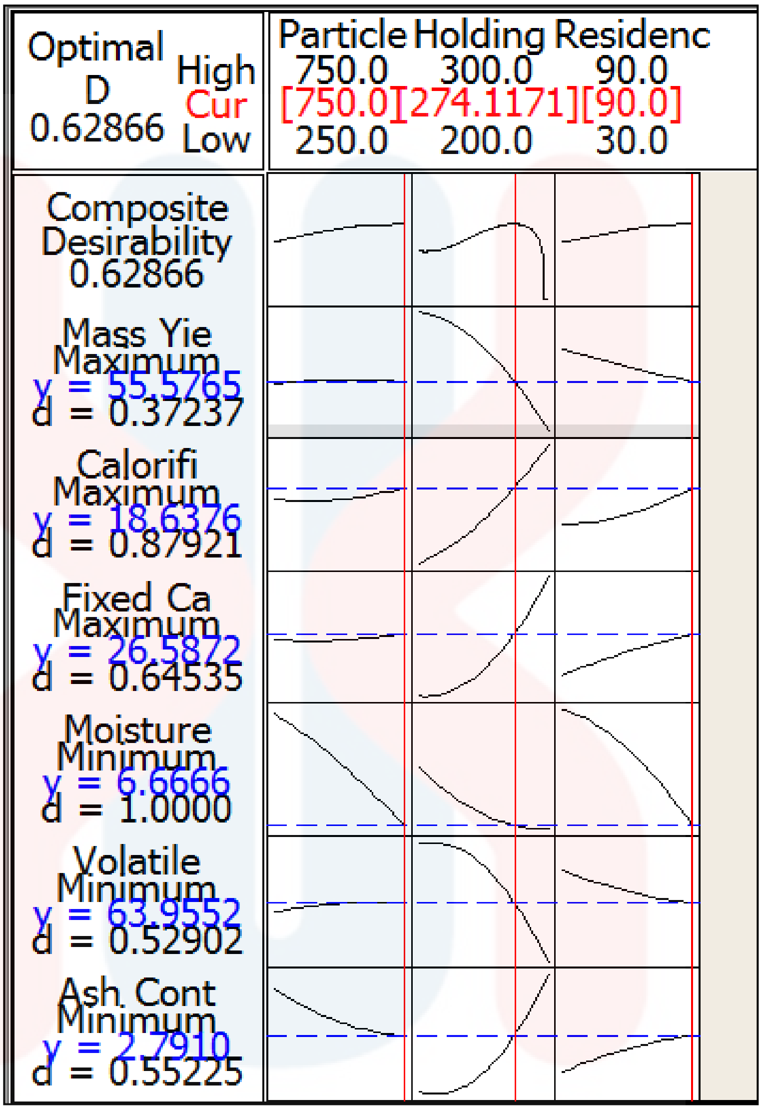

Figure 4.31: Optimization plot of all six responses

The y-value of calorific value showed that the optimum value was 18.64 MJ/kg at particle size 750 µm, holding temperature 274.12°C and residence time of 90 minutes. The particle size showed a small change of positive slope as the size increased. Holding temperature gave a very significant change on the calorific value as the temperature increase due to the steep positive slope. Holding temperature contributed to the increased of calorific value in the torrefied biochar. Residence time also showed a positive slope and as the time increased, the calorific value was slightly increased.

The y-value of fixed carbon showed that the optimum value was 26.59% at particle size 750 µm, holding temperature 274.12°C and residence time of 90 minutes. There is no visible change in fixed carbon as the particle size increased. While holding temperature showed a significant change on the fixed carbon as the temperature increased. The holding temperature had a very steep positive slope. The increased of temperature, increased the fixed carbon value. Fixed carbon also showed a positive slope as the time increased. The value of fixed carbon increased slightly as the time increased.

The y-value of moisture content showed that the optimum value was 6.67% at particle size 750 µm, holding temperature 274.12°C and residence time of 90 minutes. All the three factors showed a very visible changes since they showed a steep negative slope which indicated as the size increased, temperature increased, and time increased, the value of moisture content was decreased significantly.

The y-value volatile matter showed that the optimum value was 63.96% at particle size 750 µm, holding temperature 274.12°C and residence time of 90 minutes. Particle size showed a slightly increasing slope of volatile matter as the size increased. Holding temperature showed a very steep negative slope as time temperature increased. It indicated that as the temperature increased, the value volatile matter was decreased. Residence time also showed a negative slope. As the time increased, the volatile matter was decreased.

The y-value of ash content showed that the optimum value was 2.79% at particle size 750 µm, holding temperature 274.12°C and residence time of 90 minutes. Particle size showed a negative slope which the value of ash content decreased as the size increased. Holding temperature showed a steep positive slope as the temperature increased indicated that higher temperature caused higher ash content. Residence time showed a positive slope which contributed to the increased of ash content as the time of torrefaction increased.

The fixed carbon, ash content and calorific value increased with the torrefaction temperature and time while the volatile matter content, mass yield and moisture content were decreased (Nobre *et al.*, 2015). Ash content of the biochar targeted to be minimized since it will lower the calorific value and the carbon content of the torrefied biochar. As a result of the torrefaction process, volatile matter decreased and fixed carbon and ash content increased. As measured from the proximate analysis these improvements were proportional to the temperature and residence time and led to an increase in the torrefied OPEFB value. The increase in fixed carbon and ash content leads to a concentration of these components in the torrefied OPEFB biochar as more volatile components are removed.

Thus, the results showed that in order to receive an optimal value of factor for each of the responses, they need to obey the composite desirability. It proves that the changes in particle size do not give a significant impact on the results of the responses.

Meanwhile, holding temperature gives a significant impacts plot-based response. The changes in holding temperature gave significant changes based on the gradient of the slope. To obtain an optimal result, the suggested composite desirability was 0.62886 to generate an optimal torrefied biochar.

CHAPTER 5

CONCLUSION AND RECOMMENDATION

5.1 Conclusion

The torrefied OPEFB biochar had been successfully analysed by using an experimental design of response surface methodology (RSM), Box-Behnken design according to the OPEFB particle size, holding temperature and residence time of torrefaction process. The RSM analysis was selected based on the method's ability to separately analyse each of the variables.

The optimized torrefied OPEFB biochar had been successfully identified based on the six responses of mass yield, calorific value, fixed carbon, moisture content, volatile matter and ash content. The study proved that the holding temperature was found to exhibit the most significant effect on the responses. Based on the optimization plot, the optimal value of the responses in regards of factors that applied at 750µm of particle size, 274.12°C of holding temperature and 90 minutes of residence time, the maximum mass yield can be obtained was 55.58%. In the other hand, the maximum value of calorific value and fixed carbon were 18.64MJ/kg and 26.59% respectively. Meanwhile, the minimum value of moisture content volatile matter and ash content were 6.67%, 63.96% and 2.79% respectively.

5.2 Recommendations

Based on this study, several suggestions were suggested to be strengthened for the future study. First, there are various types of oil palm plantation waste that also contain high fibre composition such as oil palm trunk (OPT), palm kernel shell (PKS) and oil palm fronds (OPF). It is suggested that other oil palm waste should be torrefied as a source of biomass. Thus, the optimal value of OPEFB will be compared with the rest of the oil palm waste.

Second, particle size does not give much significant impacts on the torrefied OPEFB biochar optimal value. The recommendation is to consider other factors that are relevant to the independence variables which provide important results. It will thus be able to increase the validity of the experiment.

REFERENCES

Abas, R., Kamarudin, M. F., Nordin, A., & Simeh, M. A. (2011). A Study on the Malaysian Oil Palm Biomass Sector – Supply and Perception of Palm Oil Millers. *Oil Palm Industry Economic Journal*, *11*(1), 28–41.

Abdullah, N., & Sulaim, F. (2013). The Oil Palm Wastes in Malaysia. *Biomass Now - Sustainable Growth and Use*, (March). https://doi.org/10.5772/55302

Abdullah, N., Sulaiman, F., & Gerhauser, H. (2011). Characterisation of Oil Palm Empty Fruit Bunches for Fuel Application, *22*(1), 1–24.

Acharya, B., Sule, I., & Dutta, A. (2012). A review on advances of torrefaction technologies for biomass processing. *Biomass Conversion and Biorefinery*, *2*(4), 349–369. https://doi.org/10.1007/s13399-012-0058-y

Awang, A. H., Abdulrazik, A., Noor, A. M., & Nafsun, A. I. (2019). Modelling and optimization of torrefied pellet fuel production. *Pertanika Journal of Science and Technology*, *27*(4), 2139–2152.

BP. (2018). 67 th edition. *Statistical Review of World Energy*, 1–56.

BP. (2016). Statistical Review of World Energy.

Drahansky, M., Paridah, M. ., Moradbak, A., Mohamed, A. ., Owolabi, F. abdulwahab taiwo, Asniza, M., & Abdul Khalid, S. H. . (2016). We are IntechOpen , the world ' s leading publisher of Open Access books Built by scientists , for scientists TOP 1 %. *Intech*, *i*(tourism), 13. https://doi.org/http://dx.doi.org/10.5772/57353

Faizi, M. K., Shahriman, A. B., Majid, M. S. A., Shamsul, B. M. T., & Ng, Y. G. (2017). An overview of the Oil Palm Empty Fruit Bunch (OPEFB) potential as reinforcing fibre in polymer composite for energy absorption applications, *01064*.

Ferreira, S. L. C., Bruns, R. E., Ferreira, H. S., & Matos, G. D. (2007). Box-Behnken design : An alternative for the optimization of analytical methods Box-Behnken design : An alternative for the optimization of analytical methods, (October 2017). https://doi.org/10.1016/j.aca.2007.07.011

Eurostat. (2017). *Energy from renewable sources*. Retrieved December 22, 2019, from Eurostat Statistics Explained: https://ec.europa.eu/eurostat/statistics-explained/index.php/Energy_from_renewable_sources

ExxonMobile. (2018). Outlook for Energy : A View to 2040.

Goleman, daniel; boyatzis, Richard; Mckee, A. (2019). Peninsular Malaysia Electricity Supply Outlook 2017. *Journal of Chemical Information and Modeling*, *53*(9), 1689–1699. https://doi.org/10.1017/CBO9781107415324.004

Gronnow, M. J., Budarin, V. L., Mašek, O., Crombie, K. N., Brownsort, P. A., Shuttleworth, P. S., Clark, J. H. (2013). Torrefaction/biochar production by microwave and conventional slow pyrolysis - comparison of energy properties. *GCB Bioenergy*. https://doi.org/10.1111/gcbb.12021

He, Z., Wang, J., Oh, J., & Park, S. H. (2010). Robust optimization for multiple responses using response surface methodology, (May 2009), 157–171. https://doi.org/10.1002/asmb

Huang, Y. F., Cheng, P. H., Chiueh, P. Te, & Lo, S. L. (2017). Microwave Torrefaction of leucaena to Produce Biochar with High Fuel Ratio and Energy Return on Investment. In *Energy Procedia*. https://doi.org/10.1016/j.egypro.2017.03.276

Islam, A., Alam, R., & Hannan, O. (2012). Composites : Part B Multiresponse optimization based on statistical response surface methodology and desirability function for the production of particleboard. *Composites Part B*, *43*(3), 861–868. https://doi.org/10.1016/j.compositesb.2011.11.033

Kamimoto, M. (2006). The Significance of Liquid Fuel Production from Woody Biomass.

Karthikeyan, M. (2008). Minimization of moisture readsorption in dried coal samples. *Drying Technology*, *26*(7), 948–955. https://doi.org/10.1080/07373930802142846

Lin, Y.-L. (2015). Effects of Microwave — Induced Torrefaction on Waste Straw Upgrading. *International Journal of Chemical Engineering and Applications*, *6*(6), 401–404. https://doi.org/10.7763/IJCEA.2015.V6.518

Md Arshad, S. H., Ngadi, N., Wong, S., Saidina Amin, N., Razmi, F. A., Mohamed, N. B., … Abdul Aziz, A. (2019). Optimization of phenol adsorption onto biochar from oil palm empty fruit bunch (EFB). *Malaysian Journal of Fundamental and Applied Sciences*, *15*(1), 1–5. https://doi.org/10.11113/mjfas.v15n2019.1199

Ministry of Energy, G. T. and W. (2017). *Green Technology Master Plan Malaysia 2017 - 2030*. https://doi.org/ISBN NO. 978-967-5893-09-4

Nobre, C., Gonçalves, M., Mendes, B., Vilarinho, C., & Teixeira, J. (2015). Torrefaction effects on composition and quality of biomass wastes pellets. *Wastes: Solutions, Treatments and Opportunities - Selected Papers from the 3rd Edition of the International Conference on Wastes: Solutions, Treatments and Opportunities, 2015*, (September), 171–176. https://doi.org/10.1201/b18853-30

Omar, Q., Mukhtar, A., Shafiq, U., & Awan, J. A. (2017). Proximate Analysis of Low and High Quality Pure Coal and their Blends from Pakistan, (January), 2–5.

Pulka, J., Manczarski, P., Koziel, J. A., & Białowiec, A. (2019). Torrefaction of sewage sludge: Kinetics and fuel properties of biochars. *Energies*, *12*(3), 1–10. https://doi.org/10.3390/en12030565

Ranganadham, M. V. S. (2018). Energy Statistics, 101. Retrieved from http://mospi.nic.in/sites/default/files/publication_reports/Energy_Statistics_201

8.pdf

Ribeiro, J. M. C., Godina, R., Matias, J. C. de O., & Nunes, L. J. R. (2018). Future perspectives of biomass torrefaction: Review of the current state-of-the-art and research development. *Sustainability (Switzerland)*. https://doi.org/10.3390/su10072323

Saadon, S., Uemura, Y., & Mansor, N. (2014). Torrefaction in the Presence of Oxygen and Carbon Dioxide: The Effect on Yield of Oil Palm Kernel Shell. *Procedia Chemistry*. https://doi.org/10.1016/j.proche.2014.05.023

Samsudin M. S. N., Rahman M. M., M. A. W. (2016). Power Generation Sources in Malaysia : Status and Prospects for Sustainable Development. *Journal of Advanced Review on Scientific Research*, *25*(September), 11–28. https://doi.org/10.1007/s40899-015-0029-0

Senaras, A. E. (2019). Parameter optimization using the surface response technique in automated guided vehicles, 187–197. https://doi.org/10.1016/B978-0-12-816564-5.00008-6

Shafie, S. M., Mahlia, T. M. I., Masjuki, H. H., & Andriyana, A. (2011). Current energy usage and sustainable energy in Malaysia: A review. *Renewable and Sustainable Energy Reviews*, *15*(9), 4370–4377. https://doi.org/10.1016/j.rser.2011.07.113

Speight, J. G. (2015). *8 - Assessing fuels for gasification: analytical and quality control techniques for coal*. *Gasification for Synthetic Fuel Production*. © 2015 Woodhead Publishing Limited. All rights reserved. https://doi.org/10.1016/B978-0-85709-802-3.00008-4

Statistics, E. (2018). 2017 Malaysia Energy Statistics Handbook, 86. Retrieved from http://www.statcan.gc.ca/pub/57-601-x/57-601-x2012001-eng.pdf%5Cnpapers2://publication/uuid/792EFC7D-A6CF-40B5-A139-8FA59714AA41

Suhaimi, M., & Ahmad, B. (2013). Renewable Energy in Malaysia : Strategies and Development, *2*(1), 51–66. https://doi.org/10.5296/emsd.v2i1.3197

Tan, C. S. (2018). Electricity energy outlook in Malaysia Electricity energy outlook in Malaysia, (March), 1–6. https://doi.org/10.1088/1755-1315/16/1/012126

Taylor, P., Shah, H. K., Montgomery, D. C., & Carlyle, W. M. (n.d.). Response Surface Modeling and Optimization in Multiresponse Experiments Using Seemingly Unrelated Regressions Response Surface Modeling and Optimization in Multiresponse, (June 2013), 37–41. https://doi.org/10.1081/QEN-120027941

Tumuluru, J. S. (2015). Comparison of Chemical Composition and Energy Property of Torrefied Switchgrass and Corn Stover. *Frontiers in Energy Research*, *3*(NOV). https://doi.org/10.3389/fenrg.2015.00046

Verbruggen, A., Fischedick, M., Moomaw, W., Weir, T., Nadaï, A., Nilsson, L. J., Sathaye, J. (2010). Renewable energy costs, potentials, barriers: Conceptual issues. *Energy Policy*, *38*(2), 850–861.

https://doi.org/10.1016/j.enpol.2009.10.036

Version, O., Updated, O. F., & Reprint, T. O. F. (2016). Act 725 RENEWABLE ENERGY ACT 2011, (January).

Yin, G., & Dang, Y. (2008). Optimization of extraction technology of the Lycium barbarum polysaccharides by Box – Behnken statistical design, *74*, 603–610. https://doi.org/10.1016/j.carbpol.2008.04.025

Zheng, Y., Tao, L., Yang, X., Huang, Y., Liu, C., Gu, J., & Zheng, Z. (2017a). Effect of the Torrefaction Temperature on the Structural Properties and Pyrolysis Behavior of Biomass. *BioResources*, *12*(2). https://doi.org/10.15376/biores.12.2.3425-3447

Zheng, Y., Tao, L., Yang, X., Huang, Y., Liu, C., Gu, J., & Zheng, Z. (2017b). *Torrefaction temperature*. *BioResources* (Vol. 12).

APPENDIX-A

Table A.1: The experimental design for RSM

Std	Run	Factor A Particle Size (μm)	Factor B Holding Temperature (°C)	Factor C Residence Time (min)
15	1	500	250	60
4	2	750	300	60
6	3	750	250	30
16	4	500	250	60
1	5	250	200	60
2	6	750	200	60
5	7	250	250	30
12	8	500	300	90
7	9	250	250	90
13	10	500	250	60
17	11	500	250	60
3	12	250	300	60
8	13	750	250	90
9	14	500	200	30
11	15	500	200	90
10	16	500	300	30
14	17	500	250	60

Table A.2: Mass Yield

Run	Factor A Particle size (μm)	Factor B Holding Temperature (°C)	Factor C Residence Time (min)	Initial Weight (g)	Final Weight (g)	Mass Loss (%)	Mass Yield (%)
1	500	250	60	5.002	4.016	19.71	**80.29**
2	750	300	60	5.000	1.836	63.28	**36.72**
3	750	250	30	5.002	4.522	9.60	**90.40**
4	500	250	60	5.002	4.428	11.48	**88.52**
5	250	200	60	5.001	4.883	2.36	**97.64**
6	750	200	60	5.001	4.864	2.74	**97.26**
7	250	250	30	5.002	4.423	11.58	**88.42**
8	500	300	90	5.001	1.598	68.05	**31.95**
9	250	250	90	5.000	3.613	27.74	**72.26**
10	500	250	60	5.002	4.006	19.91	**80.09**
11	500	250	60	5.001	4.055	18.92	**81.08**
12	250	300	60	5.001	1.753	64.95	**35.05**
13	750	250	90	5.001	3.666	26.69	**73.31**
14	500	200	30	5.001	4.894	2.14	**97.86**
15	500	200	90	5.002	4.844	3.16	**96.84**
16	500	300	30	5.000	2.522	49.56	**50.44**
17	500	250	60	5.001	4.044	19.14	**80.86**

Table A.3: Proximate Analysis

Run	Factor A Particle Size (µm)	Factor B Holding Temperature (°C)	Factor C Residence Time (min)	Moisture Content (%)	Volatile Matter (%)	Ash Content (%)	Fixed Carbon (%)
RAW	500	-	-	**13.88**	**81.54**	**0.30**	**4.28**
1	500	250	60	**9.59**	**77.12**	**1.79**	**11.50**
2	750	300	60	**8.46**	**51.53**	**3.98**	**36.03**
3	750	250	30	**10.76**	**79.81**	**1.48**	**7.95**
4	500	250	60	**9.65**	**76.89**	**1.82**	**11.64**
5	250	200	60	**10.86**	**81.91**	**1.36**	**5.87**
6	750	200	60	**9.29**	**81.75**	**1.44**	**7.52**
7	250	250	30	**7.82**	**81.80**	**2.02**	**8.36**
8	500	300	90	**7.83**	**47.77**	**4.75**	**39.65**
9	250	250	90	**9.23**	**73.70**	**2.52**	**14.55**
10	500	250	60	**9.71**	**77.04**	**1.85**	**11.40**
11	500	250	60	**9.62**	**76.98**	**1.80**	**11.60**
12	250	300	60	**11.05**	**47.34**	**5.25**	**36.36**
13	750	250	90	**7.83**	**73.70**	**1.68**	**16.79**
14	500	200	30	**11.43**	**83.24**	**1.14**	**4.19**
15	500	200	90	**9.98**	**80.40**	**1.65**	**7.97**
16	500	300	30	**9.10**	**60.62**	**3.02**	**27.26**
17	500	250	60	**9.69**	**76.73**	**1.79**	**11.79**

Table A.4: Energy Content

Run	Factor A Particle Size (µm)	Factor B Holding Temperature (°C)	Factor C Residence Time (min)	Calorific Value (MJ/kg)
1	500	250	60	**17.6998**
2	750	300	60	**18.7780**
3	750	250	30	**17.5772**
4	500	250	60	**17.7141**
5	250	200	60	**17.7622**
6	750	200	60	**17.1847**
7	250	250	30	**17.7884**
8	500	300	90	**19.1211**
9	250	250	90	**18.1672**
10	500	250	60	**17.7425**
11	500	250	60	**17.7011**
12	250	300	60	**18.2939**
13	750	250	90	**18.0437**
14	500	200	30	**17.2230**
15	500	200	90	**17.4736**
16	500	300	30	**18.3775**
17	500	250	60	**17.3328**

Table A.5: Summary

Run Order	Particle Size	Holding Temperature	Residence Time	Mass Yield	Calorific Value	Moisture Content	Volatile Matter	Ash Content	Fixed Carbon
1	500	250	60	**80.29**	**17.6998**	**9.59**	**77.12**	**1.79**	**11.50**
2	750	300	60	**36.72**	**18.7780**	**8.46**	**51.53**	**3.98**	**36.03**
3	750	250	30	**90.40**	**17.5772**	**10.76**	**79.81**	**1.48**	**7.95**
4	500	250	60	**88.52**	**17.7141**	**9.65**	**76.89**	**1.82**	**11.64**
5	250	200	60	**97.64**	**17.7622**	**10.86**	**81.91**	**1.36**	**5.87**
6	750	200	60	**97.26**	**17.1847**	**9.29**	**81.75**	**1.44**	**7.52**
7	250	250	30	**88.42**	**17.7884**	**7.82**	**81.80**	**2.02**	**8.36**
8	500	300	90	**31.95**	**19.1211**	**7.83**	**47.77**	**4.75**	**39.65**
9	250	250	90	**72.26**	**18.1672**	**9.23**	**73.70**	**2.52**	**14.55**
10	500	250	60	**80.09**	**17.7425**	**9.71**	**77.04**	**1.85**	**11.40**
11	500	250	60	**81.08**	**17.7011**	**9.62**	**76.98**	**1.80**	**11.60**
12	250	300	60	**35.05**	**18.2939**	**11.05**	**47.34**	**5.25**	**36.36**
13	750	250	90	**73.31**	**18.0437**	**7.83**	**73.70**	**1.68**	**16.79**
14	500	200	30	**97.86**	**17.2230**	**11.43**	**83.24**	**1.14**	**4.19**
15	500	200	90	**96.84**	**17.4736**	**9.98**	**80.40**	**1.65**	**7.97**
16	500	300	30	**50.44**	**18.3775**	**9.10**	**60.62**	**3.02**	**27.26**
17	500	250	60	**80.86**	**17.3328**	**9.69**	**76.73**	**1.79**	**11.79**

APPENDIX-B

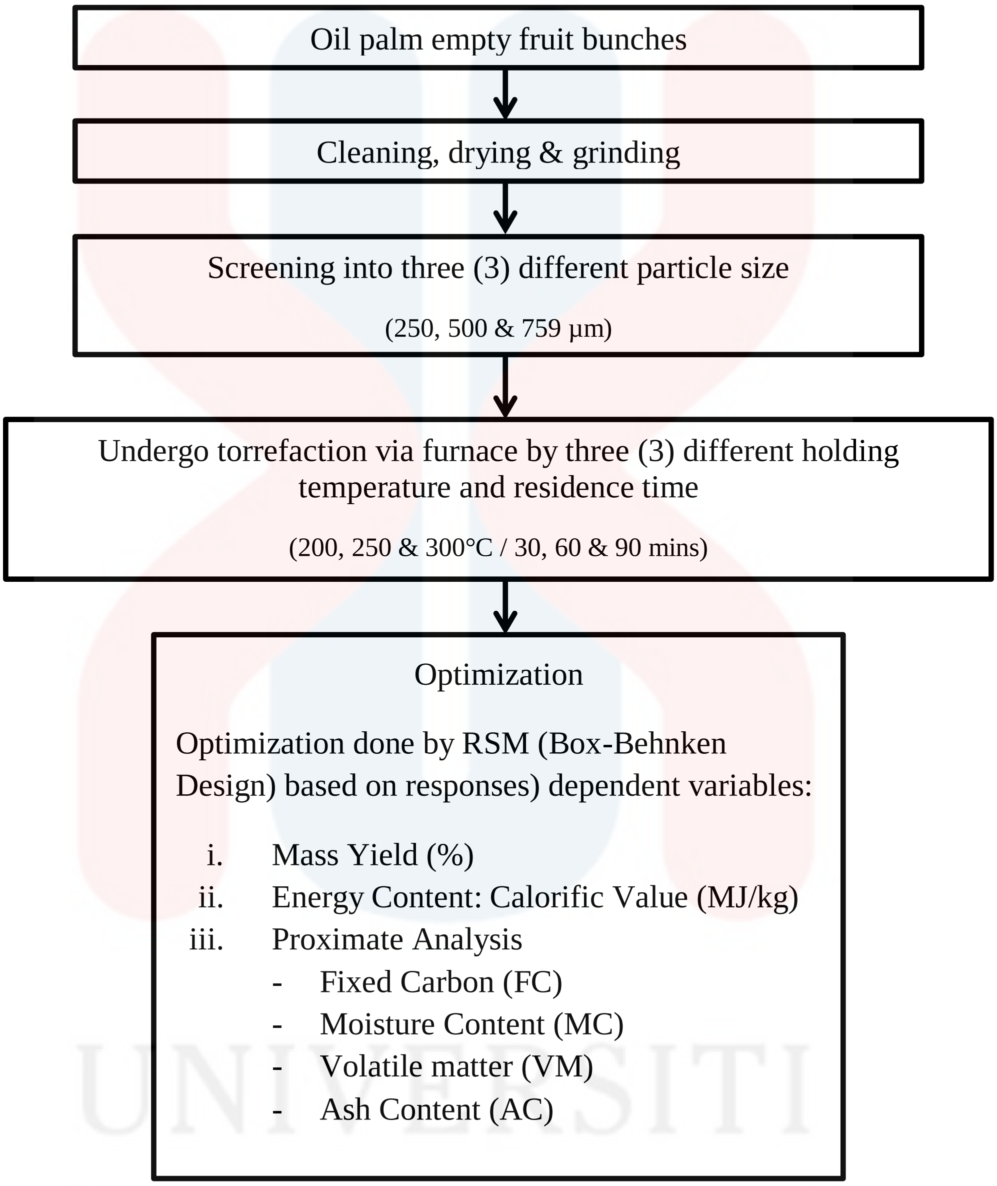

Figure B.1: Flow chart of overall process